npj | parkinson's disease

Article

Published in partnership with the Parkinson's Foundation

https://doi.org/10.1038/s41531-024-00849-1

Rational selection of the monoclonal α-synuclein antibody amlenetug (Lu AF82422) for the treatment of α-synucleinopathies

Pekka Kallunki[1] ✉, Florence Sotty[1], Katarina Willén[1], Michal Lubas[1], Laurent David[1], Malene Ambjørn[1], Ann-Louise Bergström[1], Louise Buur[1], Ibrahim Malik[1], Steffen Nyegaard[1], Thomas Thiilmark Eriksen[1], Berit O. Krogh[1], Jeffrey B. Stavenhagen[1], Kathrine J. Andersen[1], Lars Ø. Pedersen[1], Ersoy Cholak[1], Edward N. van den Brink[2], Rik Rademaker[2], Tom Vink[2], David Satijn[2], Paul W.H.I. Parren[2], Søren Christensen[1], Line R. Olsen[1], Josefine N. Søderberg[1], Sandra Vergo[1], Allan Jensen[1], Jan Egebjerg[1], Pernille Gry Wulff-Larsen[1], Mikkel N. Harndahl[1], Dina S. M. Damlund[1], Kaare Bjerregaard-Andersen[1] & Karina Fog[1]

Amlenetug (Lu AF82422) is a human monoclonal antibody targeting α-synuclein in clinical development for multiple system atrophy. We describe a series of studies that characterize its functional properties and supported its selection as a viable clinical candidate. Amlenetug inhibits seeding induced in mouse primary neurons by various α-synuclein fibrillar assemblies and by aggregates isolated from MSA brain homogenate. In vivo, both co-injection of amlenetug with α-synuclein assemblies in mouse brain and peripheral administration inhibit α-synuclein seeding. Amlenetug inhibits uptake of α-synuclein seeds as well as accumulation of C-terminal truncated α-synuclein seeds and demonstrates binding to monomeric, aggregated, and truncated forms of human α-synuclein. The epitope of amlenetug was mapped to amino acids 112-117 and further characterized by crystallographic structure analysis. Based on our data, we hypothesize that targeting α-synuclein will potentially slow further disease progression by inhibiting further pathology development but be without impact on established pathology and symptoms.

Parkinson's disease (PD), dementia with Lewy bodies (DLB) and multiple system atrophy (MSA) are progressive neurodegenerative disorders, defined by specific localizations of pathological α-synuclein (α-syn) aggregates in the brain and collectively referred to as α-synucleinopathies. PD and DLB are characterized by neuronal Lewy bodies (LBs) and Lewy Neurites (LNs), while MSA is characterized by glial cytoplasmic inclusions (GCIs)[1–3] as well as neuronal cytoplasmic and nuclear inclusions (NCIs and NNIs)[4,5]. α-Syn is the primary protein component of both LBs and GCIs[6,7]. *Postmortem* studies of PD brains have shown that the distribution of pathological aggregates either spread in a caudo-rostral anatomical pattern or in an amygdala-centered pattern[8,9]. Similarly, in MSA, it has been shown that the pathologic burden and spread increases with disease progression[10]. This pathological spread, together with the observation that heterologous fetal grafts implanted in the striatum of PD patients developed α-syn aggregates 4–10 years after grafting[11], has led to the hypothesis that α-syn oligomeric or higher aggregated species are either secreted from cells and/or released from dying cells, and taken up in connected cells where they seed pathology via a prion-like mechanism. The functional cellular and behavioral consequences of α-syn misfolding and aggregation have been widely studied and shown to result in both cellular dysfunctions, toxicity, and behavioral deficits[12].

A substantial amount of evidence from experimental models indicates that α-syn may behave in a prion-like fashion. In both animal and cellular models, addition of small amounts of aggregated α-syn preparations to the media, or injected into the brain induces the formation (seeding) of new intracellular α-syn aggregates[13–16]. In these models, the induced intracellular aggregation of α-syn does not result in morphologically fully formed, round and dense Lewy bodies similar to those in human brains. They, however, do display many similarities such as fibrillar ultrastructure, thioflavin reactivity,

[1]H. Lundbeck A/S, Research, Ottiliavej 9, 2500 Valby, Denmark. [2]Genmab, Uppsalalaan 15, 3584 CT, Utrecht, The Netherlands.
✉e-mail: PEKA@Lundbeck.com

hyper-phosphorylation at α-syn serine-129 (S129), reduced solubility, ubiquitination, truncations and even recruitment of organelles, such as mitochondria, autophagosomes and membranous vesicular structures[17]. In addition to the formation of LB-like inclusions in the cell body, the neuronal seeding models develop neuritic pathology, with abundant aggregates that are reminiscent of LNs. In the animal models, it has been shown that α-syn pathology is transmitted to neurons directly connected to the injection site, but also over time to neurons that are not directly connected[18], resembling the spreading of pathology in human brain.

Recent insights into the molecular structure of α-syn fibrillar assemblies have revealed that several distinct folds exist which may lead to assemblies with distinct properties. Such distinct folds have not only been found in in vitro generated assemblies from recombinant α-syn, but more recently also in ex vivo samples from cases of α-synucleinopathies[19]. In particular α-syn aggregates derived from MSA brains have been demonstrated to contain the highest activity in seeding assays[20], while aggregates from DLB and PD brains contain less seeding activity[21]. These findings open the possibility that different α-synucleinopathies are caused by conformationally different α-syn aggregates, commonly referred to as different strains or conformers[22,23]. Some of the most well characterized in vitro preparations of α-syn strains are preformed fibrils (PFFs)[24], fibrils[25], ribbons[25], and P91[26], and for example, injection of fibrils and ribbons in rodent brain is reported to cause α-syn pathology in different cell types and brain regions[27–29] supporting the hypothesis that conformational differences could drive specific pathologies.

Adding to the complexity of formation of α-syn aggregates is the role of post-translational modifications (PTMs) that may be tied to pathology development[30]. These may be modifications such as acetylation, phosphorylation, and nitration, or it may be truncations through protease activity. While many PTMs on α-syn have been identified, they vary in prevalence. The most well characterized PTM is the phosphorylation of S129[31] which is commonly used as a marker for pathological α-syn aggregates in vitro and in vivo.

α-Syn truncations are common phenomena and found in brain samples both from cases of PD as well as controls[32]. Both N-terminal and C-terminal truncations (CTTs), including 5-140, 1–119 and 1–122, were shown to be increased in SDS-soluble fractions of PD brain tissue[32,33] and specific antibodies against CTTs 119 and 122 have been used to show that the two CTT proteoforms mainly localize towards the core of LBs, with little staining of neuropil structures[34]. The observation that CTTs were mainly restricted to pathology-associated structures in PD patients suggests a potential role of CTT α-syn in driving α-syn aggregation and fits with in vitro and in vivo data showing increased propensity for aggregation and toxicity of CTT α-syn proteoforms[35,36].

The central role of α-syn aggregation in the pathophysiology of α-synucleinopathies has led academic research and pharmaceutical companies to pursue various ways of targeting α-syn. In 2011, the first paper was published on a potential therapeutic effect of α-syn antibodies and α-syn immunization in an animal model[37] (reviewed in refs. 38,39). Today several of these principles have entered clinical trials, including therapeutic monoclonal antibodies such as PRX-002 (prasinezumab, Roche/Prothena[40,41], BIIB054 (cinpanemab, Biogen)[42], BAN0805 (ABBV-0805, BioArctic)[43] and Lu AF82422 (amlenetug, H. Lundbeck A/S)[44], as well as vaccines such as ACI-7104/PD03A (AC Immune/Affiris)[45]. Other principles directly modulating α-syn oligomers such as Anle138b (MODAG Gmbh)[46] or directly reducing α-syn expression, such as antisense oligonucleotide BIIB101 (Ionis/Biogen)[47] are also in development.

Clinical data from phase II studies have been reported for two of the antibody-based therapies. Prasinezumab[40,41], while not meeting the primary endpoint (changes from baseline in the sum of scores of part I, I and III of the Movement Disorders Society-Unified Parkinson's Disease Rating Scale [MDS-UPDRS]) in early-stage PD, is still in clinical development, whereas Biogen has decided to discontinue cinpanemab as it did neither meet its primary (changes from baseline in the MDS-UPDRS) nor secondary endpoints (MDS-UPDRS subscale scores and DaT-SPECT) in PD[42]. Understanding the differences of these antibodies including their mechanisms of actions are extremely valuable for the field as it will support interpretations of the clinical trials, guide future decisions and inform the design and development of new and improved antibodies.

Here we report on the rationale behind selecting Lu AF82422, a human monoclonal antibody targeting α-syn, as a candidate for further development. The data supporting Lu AF82422 includes structural understanding of the epitope, binding affinities, and functional effects in cellular and mice models of seeded α-syn pathology. We also compare Lu AF82422 to prasinezumab and cinpanemab to understand the differences of the α-syn targeting antibodies and their efficacy in preclinical models.

Materials and methods

Expression and purification of full length and truncated forms of α-syn produced in eukaryotic and prokaryotic hosts

Full length, human α-syn (uniprot ID: P37840) was expressed in HEK293-6E suspension cultures and captured by anion exchange chromatography directly from the cell-free supernatant[48]. The eluate peak, was subjected to ammonium sulfate (AMS) precipitation by 40% w/v AMS for 30 min followed by 30 min centrifugation at 4500 × *g*. The pellet was solubilized in 20 mM piperazine pH 5.5 and centrifuged for 30 min at 12,000 × *g*. The supernatant was subjected to anion exchange chromatography and eluted with a NaCl gradient 0–500 mM over 10 column volumes. The eluate peak was concentrated and loaded onto a Superdex 75 column for size-exclusion chromatography (SEC). The monomeric peak fractions were pooled and concentrated to 6 mg/mL for storage at −80 °C. Final purity was assessed by SDS-PAGE and analytical SEC. Endotoxin levels were verified to be below 0.5 EU/mg. Furthermore, dynamic light scattering (DLS) was used to verify monodispersity.

Additionally, human α-syn was also expressed in *E. coli*. The sequence encoding full-length α-syn was cloned into the pET-22b vector and transformed into BL21 cells and expression induced overnight at 20 °C with 0.5 µM IPTG. Following cell harvest, the cells were resuspended in 20 mM Tris-HCl 7.6, 25 mM NaCl and 1x Complete protease inhibitor (Roche). The cells were lysed by sonication, boiled for 15 min, and then cleared by centrifugation at 12,000 × *g* for 30 min. α-syn was captured by anion exchange chromatography and eluted with a NaCl gradient 0–1 M NaCl over 20 column volumes. Fractions containing α-syn were pooled and concentrated prior to SEC on a Superdex 75 column equilibrated in PBS. Fractions containing α-syn were collected and applied to a high-capacity endotoxin removal spin column (Pierce). The monomeric peak fractions were pooled and concentrated to 5 mg/mL for storage at −80 °C. Endotoxin level was verified below 1.0 EU/mg. SEC and DLS analyses were done to verify monomeric state and monodispersity of the pure α-syn.

The truncated α-syn containing amino acids 1-119 was produced in *E. coli*. The sequence encoding the protein fragment fused N-terminally to a factor Xa cleavage site and hexa-His tag was cloned into the pET24a(+) expression vector (Novagen). The plasmid vector was transformed into *E. coli* BL21 for expression using the overnight express autoinduction system (Novagen). Cells were harvested and lyzed prior to capture on a 5 ml HisTrap column (GE HealthCare) equilibrated in 20 mM Sodium phosphate pH 7.5, 1 M NaCl (buffer A). Elution was done in a gradient to 0.25 M imidazole in buffer A over 20 column volumes. Further purification was done by size exclusion on a S200 (26/60) column (GE HealthCare) in 10 mM Tris pH 7.4, 300 mM NaCl. To remove the N-terminal tag, the purified His-tagged α-syn 1-119 was incubated with factor Xa in a 1:50 ratio. The cleaved α-syn 1-119 was collected from the HisTrap flow through and concentrated to app. 400 µg/ml using a Centricon concentration device.

For assessment of antibody cross-reactivity and selection/deselection, full length mouse, rat and cynomolgus monkey α-syn, as well as human β-synuclein and γ-synuclein, were produced. The proteins were designed with a C-terminal Biotin acceptor peptide (BAP) tag and expressed together with BirA biotin ligase enzyme for intra-cellular biotinylation. Mammalian expression vectors were constructed carrying the different α-syn + BAP tag fusion constructs and expressed in HEK 293 cells using transient

transfection (Genmab BV)[49]. The various synuclein proteins were purified directly from the media.

Generation of α-syn fibrillar assemblies

To prepare fibrillar assemblies for in vitro and in vivo seeding models, monomeric α-syn (from HEK293) was thawed and diluted to 4 mg/mL in PBS. The thawed monomer was verified to be free of aggregates by DLS. The solution was then transferred to round bottom tubes sealed with parafilm and placed in an orbital shaker for 5 days at 37 °C and 1000 rpm. The PFFs were sonicated for 10 min with cycles of 20 s on and 10 s off at 50% amplitude (Q800R3, Qsonica) and sonicated PFFs were aliquoted in volumes of 10 µL and stored at −80 °C. Different strains of α-syn fibrillar assemblies for in vitro and in vivo experiments were generated according to protocols available in literature that describes the formation of PFFs[25], Fibrils[25], Ribbons[25], and P91[26]. The α-syn monomeric protein (full length or 1-119) was transferred to a suitable buffer to prepare a given strain. For PFFs: 1x PBS (Gibco). For Fibrils: 50 mM Tris-HCl pH 7.5, 150 mM KCl. For Ribbons: 5 mM Tris-HCl pH 7.5. For P91: 20 mM K_3PO_4 pH 9.1. The α-syn was subjected to agitation at 1000 rpm at 37 °C in a Thermomixer (Thermo Fisher) for 7 days to facilitate fibrillation. The products were then sonicated using a Q800R2 water batch sonicator (QSonica) to maintain 20 °C during the process. Sonication was carried out for 10 min at 50% amplitude with cycles 20 s on, 1 s off. Finally, the produced assemblies were aliquoted to 10 µl and frozen at −80 °C until use. Prior to use, aliquots were thawed in water bath at 20 °C and kept at RT. Formation of fibrillar assemblies was verified by increase in thioflavin T fluorescence. The Z-average size and polydispersity index (PDI) was determined following sonication. In general, a size distribution average >100 nm and a PDI > 0.2 showed good correlation to seeding potency in vitro. Data characterizing fibrillar assemblies and representative images are summarized in Supplementary Fig. 1.

Fibrillar assemblies for immunization were made from full length, recombinant α-syn (*E. coli* derived) purchased from Rpeptide (US) as lyophilized product. This was dissolved in 20 mM Tris-HCl pH 7.5, 300 mM NaCl at 1 mg/ml protein. The solution was incubated 170 µl aliquots in 96 well plate with a 70 µm diameter ceramic bead in each well at 200 rpm in Vortemp 56 shaker incubator (Labnet International), at 37 °C for 7 days. The formation of fibrils was followed by fluorescence increase trough the addition of thioflavin T in one of the wells.

Mouse immunizations, selection, and expression of antibodies

Antibodies were produced by immunizations of the transgenic HuMAb mouse strains HCo17-BALB/c and HCo12-BALB/c mice, which carry a (partial) human immunoglobulin repertoire and are used for raising and isolating human monoclonal antibodies. The mice were immunized with three immunogens in a protocol first using human full length α-syn-fibrils followed by C-terminal truncated monomers: α-syn 1-60 (Rpeptide, US) in week 2 (boost 1) and α-syn 1-119 in week 6 (boost 2). Additional boost (3–6) was done with human full length α-syn-fibrils on a bi-weekly schedule. The first immunization was performed with α-syn immunogens in complete Freund's adjuvant (CFA; Difco Laboratories, Detroit, MI, USA), followed by boosting in incomplete Freund's adjuvant (IFA). Serum titers were screened bi-weekly using biotin-tagged human α-syn (dilution of serum of 1/50) and mice selected for hybridoma fusion if titers were positive on at least two sequential, biweekly, screening events.

Hybridomas were produced and supernatants were selected for binding to human α-syn. For each hybridoma, 16 VL and VH sequences were obtained and the productive VH-VL combination identified by co-expression in HEK293 cells. The recombinantly expressed antibodies were further characterized for binding to mouse, rat and cynomolgus monkey α-syn and de-selected for binding to β-synuclein and γ-synuclein. Specificity to human α-syn was confirmed using Octet 384RED (Fortebio, Menlo Park, USA), with purified antibodies at 2 µg/ml. The raw data from Octet is included in Supplementary File 1.

Lu AF82422, a monospecific wild type human IgG1, was expressed in a CHOK1SV GS-KO cell line and purified by capture on protein A followed by an anion exchange chromatography step (Lonza, CH). The purity and monodispersity of the antibodies were assessed by SDS-PAGE and analytical SEC. Identities of Lu AF82422 was verified by mass spectrometry (MS). Fab fragments of Lu AF82422 were produced by proteolytic cleavage using the FabAlactica kit (Genovis).

Prasinezumab (PRX-002, CAS register 1960462-19-4) was produced internally at H. Lundbeck A/S. Vectors encoding prasinezumab HC and LC were produced based on the pTT5 expression plasmid[48]. Expression was done in HEK293 6E followed by affinity capture on protein G (GE healthcare) and anion exchange on Q-Sepharose (GE HealthCare). Cinpanemab (BIIB-054,CAS register 2094516-02-4) was produced internally at H. Lundbeck A/S; vectors encoding BIIB-054HC and LC were produced based on the pTT5 expression plasmid. Expression was done in HEK293 6E followed by affinity capture on protein G (GE HealthCare) and anion exchange on Q-Sepharose (GE healthcare). For both prasinezumab and cinpanemab, a single, monodisperse peak was observed. Binding of all antibodies recognizing α-syn was verified by SPR.

The VH and VL sequences for the human IgG1 isotype control antibody anti-hen egg white lysozyme (HEL), Lu AF67501, was obtained from reference[50]. The antibody was produced by Crown Bioscience (US) and purchased by H. Lundbeck A/S. The sequence for the antibody IgG1 b12/Lu AF77829 targeting HIV-1 envelope glycoprotein gp120 was obtained from reference[51]. The antibody was produced at Akesobio (CN). The antibodies were used as IgG1 isotype controls as indicated.

Sources and ethical approvals for human materials used in the study

Post-mortem human brain tissue from PD patients (putamen), MSA patients (putamen and cerebellum) DLB patients (cortex) as well as age-matched controls (putamen and cerebellum), were acquired from Tissue Solutions (UK) currently owned by BioIVT as frozen blocks. A list of samples can be found in Supplementary Table 1. The samples were collected under institutional review board (IRB) ethical approval and with informed donor consent.

Paraffin embedded blocks from human substantia nigra (2 PD patients with Lewy body pathology and 2 controls) used to generate data in Fig. 1C were also acquired from Tissue Solutions (UK) currently owned by BioIVT.

Frozen human brain tissue sections used to generate data in Fig. 3C–H were acquired by BioIVT, and the tissue was sourced from the Netherlands Brain Biobank (NBB) under their ethical approval. The CRO BioIVT (UK) has the rights to screen samples from NBB. Two patients with each disease (PD, MSA and DLB) were used for the staining.

Preparation of crude brain homogenates for immunoprecipitation

To prepare crude homogenates of brain tissue, samples were homogenized by a bead homogenizer (Precellys, Bertin Technologies) using 2 cycles of 50 s at 5000 rpm in buffer containing 20 mM HEPES pH 7.4, 1x protease inhibitors (Roche) and 1x phosphatase inhibitor (Roche). Aliquoted homogenates were stored at −80 °C. The aliquots were thawed at RT and 100 µl of crude homogenate was mixed with 2x lysis buffer (100 mM HEPES pH 7.4, 300 mM NaCl, 2% Triton X-100) in 1:1 V/V ratio. The solution was then subjected to sonication for 2 min, amplitude 90% at 4 °C using water bath sonicator (QSonica, Q800R2). Lysates were spun down at 1000 × *g* for 10 min at 4 °C and the supernatants were used for further analyses. Protein concentration was measured by Bradford and BCA assay for normalization purposes. Brain lysates were stored at −80 °C or directly analyzed.

Isolation of insoluble aggregates derived from brain tissue from cases of MSA and PD

To isolate sarkosyl insoluble material, a protocol based on the method published by Tarutani et al.[52] was used. Briefly, a 10% homogenate of each sample was

made from 200 mg of tissue in 2 mL of A68 buffer (10 mM Tris-HCl pH 7.5, 10% sucrose, 0.8 M NaCl, 1 mM EGTA, 1x protease inhibitor cocktail (Complete, Sigma), 1x phosphatase inhibitor (PhosStop, Sigma). Homogenization was done using a Precellys 24 (Bertin Instruments) at 5000 rpm, 2 cycles, 50 s on, 10 s off. The homogenates were centrifuged at 2000 × *g* for 10 min at 25 °C and the supernatants were transferred to clean vials. To each sample, sarkosyl (International Biotechnologies) were added to final concentration of 2% and incubated at 37 °C for 30 min. The samples were then centrifuged at 100,000 × *g* at 25 °C for 30 min and the resulting pellets were resuspended by pipetting in 1 mL of 1x A68 buffer. The samples were again centrifuged at 100,000 × *g* for 30 min at 25 °C. The resulting pellets were resuspended in 0.5 mL of 1xDPBS (Gibco). Finally, the samples were sonicated using a Qsonica800 (Amplitude 50%, 20 min, cycles 20 s on, 10 s off) and stored at −80 °C.

Immunochemistry on human brain sections

Cryosections (12 µm) of brain (superior temporal gyrus, locus coeruleus, cerebellum and striatum) from human patients with MSA, PD and DLB were used to test Lewy pathology staining by the α-syn antibodies. The staining was done with two patients for each brain section selected based on signal with the positive control antibody. Briefly, slides were taken out from −80 °C and left to air dry for 30 min prior to fixation with 4% PFA for 10 min. Following fixations slides were blocked with biotin/avidin/peroxidase reagents and then incubated with positive control antibody for Lewy pathology, phospho-Serine 129 α-syn antibody (pSYN#64), mIgG ascites, WAKO, #015-25191 or biotinylated α-syn antibody at a concentration of 1.25 µg/ml. The positive control antibody was detected with a secondary antibody, Mouse anti-human IgG1 isotype control, #X0931: Agilent DAKO. Biotinylated α-syn antibodies were detected directly by Vectastain® R.T.U Elite® ABC, #PK-7100, Vector laboratories and ImmPACT® DAB substrate kit- peroxidase, #SK-4105, Vector laboratories. The stained slides were digitally scanned (Aperio) for imaging of the pathology.

Immunoprecipitation of αSyn from brain lysates followed by western blotting

Dynabeads® epoxy (Thermo Fisher) were coated with Lu AF67501 (negative control) or Lu AF82422 according to manufacturer's instructions using 8 µg of antibody per mg of beads. Prior to immunoprecipitation (IP), brain lysates were diluted in 1x lysis buffer (50 mM HEPES pH7.4, 150 mM NaCl, 1% Triton X-100) using equal amount of total protein in range of 50–100 ug per IP. Beads were incubated at 4 °C with constant rotation at 15 rpm for 120 min. Unbound fractions were collected for HTRF analysis using a custom designed assay (see the section 0), and beads were subjected to three washes with 1x lysis buffer. Purified material was eluted with 1.5x NuPAGE buffer containing 10 mM DTT at 95 °C for 5 min with shaking at 1200 rpm. For western blots (WBs), the eluates were separated on 4–12% NuPAGE Bis-Tris protein gels and blotted onto PVDF membrane. Membranes were immunostained using antibodies against total α-syn (4B12, Thermo Scientific MA1-90346) and pS129 α-syn (ab51253, Abcam). The signal was quantified by an infrared fluorescence detection-based method with an Odyssey imager (LI-COR).

Syn aggregation measured with HTRF-based assay

The quantification of α-syn aggregates was performed based on the Homogeneous Time Resolved Fluorescence (HTRF) technology using reagents and protocol according to the manufacturer's instructions (Cisbio, Revity). Both a pS129 α-syn kit (*6FCUSOOO*) and a custom designed assay based on a monoclonal antibody recognizing residues 130-140 of α-syn (labeled with either Eu^{3+}-cryptate donor or d2-acceptor) was used as indicated. Plates were read on a PHERAstar microplate-reader, and the fluorescence was measured at 620 nm and 665 nm. Ratiometric calculation was applied using raw data from the plate reader. The HTRF ratio representing the signal from α-syn aggregates, was calculated using the equation: HTRF ratio = [(Signal 665 nm) / (Background 620 nm)] × 104. The ratio for each well within an assay is calculated and the mean and standard deviation of replicates are determined using these values. Mean values of three reactions from a representative experiment are plotted and error bars indicate standard deviation across replicates.

Peptide arrays for epitope mapping

To map the epitope, antibodies were tested on binding to linear overlapping peptides that cover the entire 140 aa sequence of α-syn. In addition, the effect of methionine oxidation and tyrosine nitration on antibody binding was tested by synthesizing peptides with these modifications. Synthesized peptides were 20 residues in length with an overlap of 19 residues produced by PepScan (NL). The binding of antibody to each of the synthesized peptides was tested in a PEPSCAN-based ELISA. The peptide arrays were incubated with primary antibody solution (overnight at 4 °C). After washing, the peptide arrays were incubated with a 1/1000 dilution of an antibody peroxidase conjugate (SBA, cat.nr.2010-05) for 1 h at 25 °C. After washing, the peroxidase substrate 2,2'-azino-di-3-ethylbenzthiazoline sulfonate (ABTS) and 2 µl/ml of 3% H_2O_2 were added. After 1 h, the color development was quantified with a charge coupled device (CCD)—camera and an image processing system. Raw data from the epitope mapping are available in Supplementary File 1.

Crystal structure determination of Lu AF82422 complexed with α-syn epitope

The structure of the Lu AF82422 Fab/α-syn complex was determined by X-ray crystallography. Lu AF82422 Fab and human α-syn were supplied by H. Lundbeck A/S. App. 3 mg of Lu AF82422 Fab and α-syn were mixed and incubated at 4 °C for 7 h and then loaded onto an S75 gel filtration column pre-equilibrated in 20 mM Tris pH 7.4 and 150 mM KCl. Peak fractions were selected for pooling using SDS-PAGE and the pooled complex was concentrated to 10 mg/mL prior to crystallization. The complex was co-crystallized using a Mosquito robot (SPT Labtech, UK) employing the hanging drop method of vapor diffusion in 96 well format with 1:1 ratio in 200 nL drops. Crystals appeared in 0.1 M Tris pH 8.0, 2 mM $ZnCl_2$ and 18% w/v PEG 6000. Crystals were mounted in a cryo-loop and flash-cooled 10 s transfer into a cryo-solution containing 0.08 M Tris pH 8.0, 1.6 mM $ZnCl_2$, 14.4% w/v PEG 6000 and 20% v/v glycerol and then into liquid nitrogen for storage until data collection.

Data were collected at the Diamond Light Source synchrotron at beamline I04 using a Dectris Pilatus 6M-F detector. Data processing in MOSFLM (CCP4)[53] and AIMLESS (CCP4)[54] indicated that the most likely space group was *C*2 with unit cell dimensions a = 132.5 Å, b = 59.1 Å and c = 69.1 Å. The Matthews coefficient (2.07 Å3/Da and 40.5% solvent content) indicated that there was most probably one complete α-syn-Fab complex per asymmetric unit. Models for use in molecular replacement (MR) were chosen by BLAST searching the sequences of the Fab heavy and light chain constant and variable domains against the PDB. Models with highest sequence identity were PDB ID: 2VYR (for Lu AF82422 Fab heavy chain variable domain), PDB ID: 2RCJ (for Lu AF82422 Fab heavy chain constant domain) and PDB ID: 4NP4 (for Lu AF82422 Fab light chain variable and constant domains). The elbow hinge regions between the variable and constant domains of the heavy and light chains were removed to create four separate MR search ensembles (VH, VL, CH and CL). Amino acid residues were trimmed from the CDRs (defined according to Kabat numbering) of the heavy and light variable domain models after visual inspection in COOT[55] to prevent any potential clashes in the α-syn-Fab interface that may cause MR to fail. All four of the input search ensembles (VH, VL, CH and CL) that were required to build a complete Fab were correctly located by MR using PHASER (CCP4)[56]. The MR output model was given 20 cycles of jelly body refinement using REFMAC5 (CCP4)[57]. The Fab protein sequence was mutated to match that of Lu AF82422 using CHAINSAW (CCP4). Eleven residues from α-syn were identified and added to the model and it was refined using REFMAC5 (CCP4). Water molecules were added using the water placement option in COOT[55] and refined using REFMAC5 (CCP4). The final protein model contained

A

Antibody	Human α-syn	Human β-syn	Human γ-syn	Macaque α-syn	Rat α-syn	Mouse α-syn
Lu AF55696	2.0	1.8	0.0	1.8	1.9	1.4
Lu AF55699	2.0	0.0	0.0	2.8	0.0	0.0
Lu AF82422	2.9	0.0	0.0	3.4	3.5	3.1
Lu AF55690	2.4	0.0	0.0	2.4	2.7	2.9

B

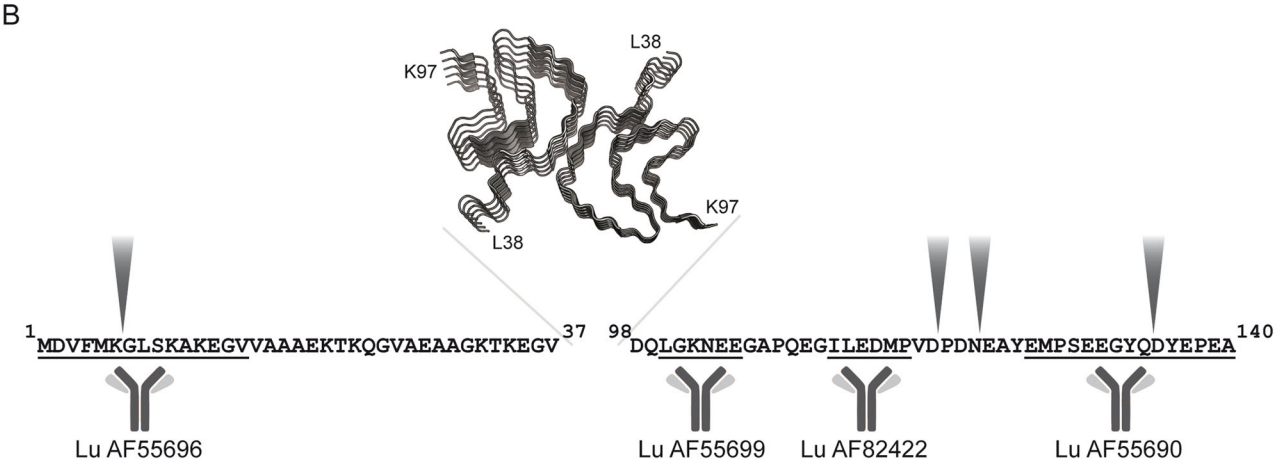

C

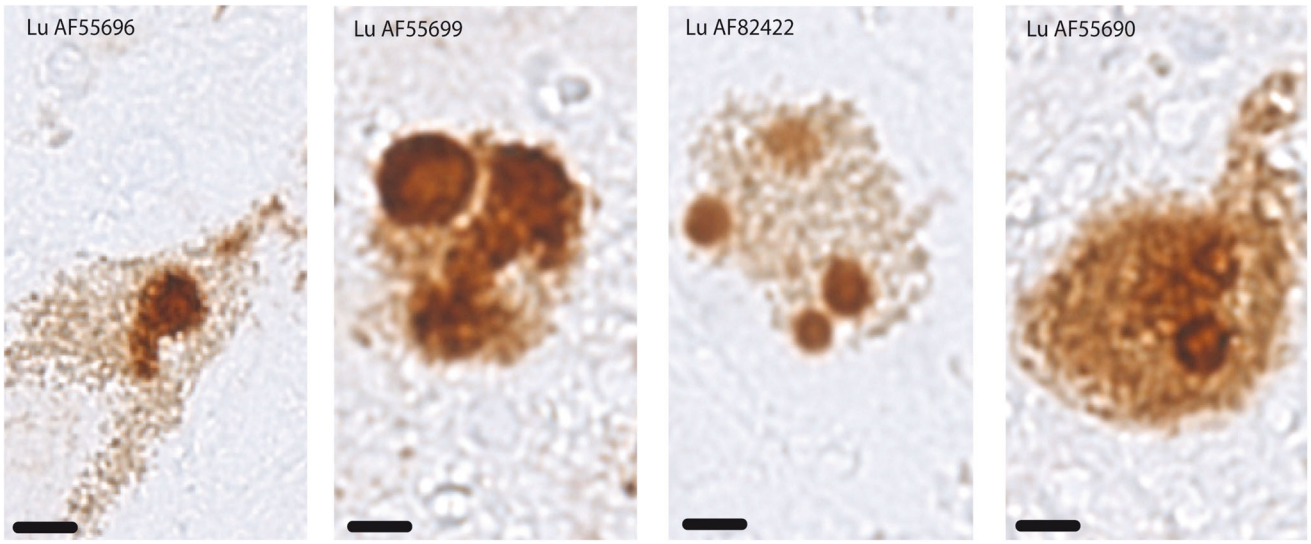

Fig. 1 | Basic binding characteristics and epitope overview of four representative antibodies identified from the immunization campaign: Lu AF55696, Lu AF55699, Lu AF82422 and Lu AF55690. A Octet binding (octet response units; nm) to human, macaque, mouse, and rat monomeric α-syn as well as human β- and γ-syn. **B** Overview of linear epitope (underlined) locations on α-syn N- and C-terminal sequences on either side of the NAC domain. Common truncation sites marked. **C** Immunohistochemical staining pattern in substantia nigra of a PD patient. Lewy Body like inclusion bodies were identified in dopaminergic neurons (neuromelanin positive brown deposits inside the cells) with all antibodies. Scalebar = 10 nm. A file containing Octet binding data and the raw data from the epitope mapping is included in Supplementary File 1.

residues 110-117 from chain A (α-syn), 1-127 and 133-214 from chain H (Lu AF82422 HC) and 1-211 from chain L (Lu AF82422 LC). The final model also contained 146 water molecules. Final R_{work} = 21.0%, R_{free} = 26.3%.

Data collection and refinement statistics are collected in Supplementary Table 2. Model coordinates and experimental structure factors of Lu AF82422 Fab/α-syn 110–117 complex have been deposited in the Protein Data Bank with the accession number 8B9V.

In silico calculation of epitope residue binding contribution by free energy perturbation

Computational alanine scanning was performed using free energy perturbation calculation (FEP). The Schrödinger FEP method, FEP+, used to estimate the relative binding free energy of protein complexes has been described and shown to outperform simpler approaches such as MM-GBSA[58–61]. FEP+ was applied to the α-syn epitope residues 110-119 of the crystallographic Lu AF82422 Fab:α-syn complex using Maestro

(Schrodinger Suite Release 2021-3 FEP+ (2021), Schrodinger L.L.C.) using the default parameters of OPLS4 force field with SPC water model. All crystallographic water molecules and ions were kept in the system.

Primary mouse neuronal cultures

Cortical neurons were prepared from wt (C57BL/6J C57BL/6JBomTac) or F28 (human α-syn-overexpressing)[62] mouse embryos at E16. In short, time pregnant mice were cervically dislocated, and embryos transferred, decapitated, and kept in ice-cold Hibernate E. Cortices were dissected and meninges removed before incubation in trypsin/EDTA/hibernate w/o $CaCl_2$ solution shaking at 37 °C for 15 min following titration in HS-MEM. Cells were plated in poly-L-lysine coated thin-bottom 96-well plates at a density of 40,000 cells/well in neuronal plating medium containing FBS. Neurons for WB experiments investigating seed truncation, were plated in 12-well plates at a density of 40,000 cells/well. After 4 h, media was exchanged to neuronal maintenance media with Neurobasal media plus and B27 plus supplement. Mitosis inhibitor Ara-C was added to a final concentration of 1 µM at 3 DIV.

Antibody inhibition of seeding in primary neurons with pS129 α-syn immunolabelling, pS129 HTRF and WB as a readout

Antibody inhibition of seeding was performed in F28 primary mouse neurons with pS129 α-syn immunolabelling as a readout for seeding. The test antibodies were diluted to a 4x final concentration in Neuronal maintenance medium in a 7-fold dilution series in a deep well plate. They were subsequently mixed with seeding material diluted to a 4x final concentration in Neuronal maintenance medium (final antibody concentrations as indicated in the respective figure texts). This mix was incubated for 15 min at RT before addition to cells at 5 DIV in a 50% media change. At 12 DIV cells were washed once with 37 °C PBS and fixed in ice cold methanol for 10 min at −20 °C, washed once in PBS and subsequently immunofluorescent labeled. Briefly, cells were labeled with pS129 α-syn (Abcam 51253) at 1:1000 dilution in PBS for 1 h at RT, then washed twice before incubation with secondary antibody donkey-anti-rabbit Cy3 (1:1000) and Hoechst (1:500) for 30 min at RT. Cells were subsequently washed twice and kept sealed with 0.2% sodium azide in PBS. pS129 α-syn and Hoechst fluorescence were read by Cellomics Array Scan VTI HCS Reader (Thermo Fisher Scientific) with a 20x objective and analyzed in Thermo Fisher Scientific HCS Studio: Cellomics Scan Version 6.6.0 (Thermo Fisher Scientific). Seeding was measured as pS129 α-syn Spot Total Intensity/viable cell count. Viable cell count was performed at a separate re-scan only counting Hoechst positive cell bodies from cells that were alive before fixation, based on nuclear size and fluorescent intensity. Each condition was measured in 6 technical replicates (wells) per culture experiment, with each well imaged in 50 fields of view with a 40x objective, corresponding to approximately 2500 viable cells. Each experiment was replicated in several cultures and normalized result was expressed as mean pS129 fluorescence/cell (% of top plateau) or mean pS129 fluorescence/cell (% of seed control) where seed control is pS129 levels without mAbs.

The pS129 α-syn HTRF assay was also used as a readout for the antibody inhibition of seeding in the F28 primary neurons. The neurons were treated at DIV5 with 0.4 µg/ml α-syn assemblies of the P91 type premixed with antibody as above. At 12 DIV cells were harvested, and seeding was analyzed with Phospho-Ser129 α-Syn aggregation Kit (*6FCUS000, Revity*). The experiment was replicated in three separate cultures and the normalized result was expressed as pS129 HTRF ratio of 665 nm/620 nm wavelengths (% of top plateau).

The ability of Lu AF82422 to inhibit seeding was also investigated in wt and F28 primary mouse neurons with fractionation and WB analysis. α-syn assemblies of the p91 type (1.5 µg/ml) were premixed with Lu AF82422 or control antibody (250 µg/ml) for 15 min and added to mouse primary cultures at DIV5. Cells were harvested for WB analysis at DIV12. Briefly, cells were washed in ice-cold PBS, collected by scraping in PBS and subsequently centrifuged at 1000 × *g* for 5 min. The pellet was resuspended in 100 µl ice-cold Triton-lysis buffer (1% Triton X-100 in 50 mM Tris, 150 mM NaCl (pH 7.6) with complete mini and phosphatase inhibitors), incubated on ice for 15 min and subsequently sonicated for 30 s. Cell lysate was centrifuged at 100,000 × *g* for 30 min at 4 °C and supernatant was kept as the Triton soluble fraction. Pellet was washed once in Triton buffer and resuspend in 100 µl SDS lysis buffer (1% SDS in 50 mM Tris, 150 mM NaCl (pH 7.6)). Samples were sonicated for 30 s, centrifuged at 100,000 × *g* for 30 min at 22 °C and supernatant was kept as the Triton insoluble/SDS soluble fraction. Protein concentrations were measured with BCA assay and 5 µg of each sample were separated on 4-12% NuPAGE Bis-Tris protein gels and blotted onto PVDF membrane that were subsequently boiled at 95 °C in PBS for 3 min. Membranes were immunostained using antibody against pS129 α-syn (Abcam, ab5125) to detect seeding and antibody against human α-syn (4B12, Thermo Fisher Scientific MA1-90346) to detect PFFs. Signal was detected by a Li-cor infrared fluorescence detection-based method with an Odyssey imager.

Determination of seed truncation in primary neuronal cultures with WB

To investigate the effect of antibodies on α-syn seed processing in cell culture, α-syn assemblies of the P91 type (1.5 µg/ml) were premixed with antibodies (250 µg/ml) and added to wt mouse primary cultures at DIV5. Cells were harvested for WB analysis after 24 h and 7 days. Cell lysates were separated on 4-12% NuPAGE Bis-Tris protein gels and blotted onto PVDF membrane that were subsequently boiled at 95 °C in PBS for 3 min. Membranes were immunostained using antibody against human α-syn (4B12, Thermo Fisher Scientific MA1-90346) to detect PFFs. Signal was quantified by a Li-cor infrared fluorescence detection-based method with an Odyssey imager. Quantification was performed in Empiria Studio (LI-COR) and normalized against internal loading control GAPDH.

Antibody inhibition of seed uptake in primary neurons

Fibrillar assemblies of the PFF-type were labeled with pHrodo iFL red STP ester (P36010, ThermoFisher) in the ratio of 0.1 mg/mL dye to 4 mg/mL PFF. The mixture was incubated and shaken at 1000x rpm for 30 min at 37 °C. Excessive dye was removed by centrifugation at 20,000 × *g* for 30 min and the supernatant discarded. The labeled PFFs were resuspended in PBS without CaCl to a final concentration of 4 mg/mL and stored at −80 °C. At the day of experiment pHrodo-PFF was mixed with antibodies (control Lu AF77829 or Lu AF82422) for 15 min in the dark before adding the mixture to the medium of F28 primary mouse cultures at DIV 5 (final antibody concentrations as indicated in the figure text). At DIV 7, cells were stained with Hoechst and live imaged at 37 °C under 5% CO2 using Cellomics Array Scan VTI HCS reader (Thermo Fisher Scientific) with the build-in software (Thermo Fisher Scientific HCS Studio: Cellomics Scan version 6.6.0 (build 5183). Briefly, the cells were detected with by Hoechst and only alive cells were analyzed. The total intensity above background was detected around alive nuclei and blotted as intensity per cell normalized to the intensity in cells treated with pHrodo-PFF only.

Antibody seeding inhibition in vivo

The animal experiments were performed in accordance with the European Communities Council Directive no. 86/609, the directives of the Danish National Committee on Animal Research Ethics, and Danish legislation on experimental animals (license no. 2014-15-0201-00339).

The ability of α-syn antibodies to inhibit seeding in vivo was first investigated in a co-injection paradigm. Briefly, α-syn assemblies of the Fibril type were mixed with antibodies at an antibody:Fibril molar ratio of 1:1, 1:3 or 1:10, between 5 and 30 min prior to intracerebral injection. The molar concentration of fibrils was based on the monomer concentration prior to fibrillation and was fixed at 133 µM (2 µg/µl). Lu AF82422 or an isotype control hIgG (Lu AF77829) were tested in this paradigm. Two µL of the antibody-fibril mix were injected in the right striatum of C57BL6JBomTac male mice (8–10 weeks of age, Taconic, Denmark) under isoflurane anesthesia at the following stereotaxic coordinates: AP + 0.5 mm, L 2.1 mm, DV 2.6 mm with reference to Bregma, as described

previously[63]. Six weeks after intracerebral injection, the animals were perfused transcardially with 4% paraformaldehyde and their brain harvested, post-fixed overnight before being transferred to PBS + 0.1% sodium azide. Immunohistochemistry for visualization of pS129 α-syn (Biotin-conjugated pSyn #64, Wako) was performed by Neuroscience Associates (Knoxville, TN, USA) using their Multi-Brain® technology. Quantification of the pS129-α-syn staining were done on the ipsilateral side of the injection and performed by manual counting of the number of positive neurons in the substantia nigra in 6 to 8 sections spaced 210 µm apart.

For assessment of the ability of Lu AF82422 to inhibit seeding in vivo after peripheral administration C57BL/6J BomTac male mice (8–10 weeks of age) were assigned to the following treatment groups: Lu AF77829 administered once weekly (100 mg/kg i.p.) from 2 weeks before and up to 6 weeks after seeding initiation; Lu AF82422 administered once weekly (100 mg/kg i.p.) from 2 weeks before and up to 6 weeks after seeding initiation; Lu AF82422 administered once weekly (100 mg/kg i.p.) from 1 week after and up to 6 weeks after seeding initiation. Seeding initiation consisted of intrastriatal injection of the more potent P91 fibrillar strain (0.25 µg in 2 µl) under isoflurane anesthesia at the same stereotaxic coordinates as described above. To measure hIgG levels in plasma, a blood sample was collected 1 week and 6 weeks after seeding initiation. Human IgG levels were measured by LC-MS. Six weeks after intracerebral injection, the animals were perfused transcardially, and immunohistochemistry was performed as described above. Quantification of the pS129-α-syn staining were done on the ipsilateral side of the injection and performed by manual counting of the number of positive neurons in the substantia nigra and motor cortex.

Mean experimental data ± standard error of the mean (SEM) was graphed using GraphPad Prism software. All statistical analyses were performed using GraphPad Prism statistical analysis software. Differences between antibody treatment groups and IgG control groups were defined as statistically significant when $p < 0.05$.

Antibody binding affinity determination with ELISA, SPR and MDS

To define the binding affinity the following experiments were performed for Lu AF82422, prasinezumab and cinpanemab. α-Syn aggregates obtained from either PD, MSA or human brains (Ctrl), α-syn assemblies of the PFF type or monomer were immobilized directly onto MSD plates. The test antibodies were titrated from 50 nM in a 6-fold dilution in deep-well plates and transferred to MSD Multi-Array 384-well Plates coated with either PD, MSA, Ctrl, PFF, monomer, or no coat in coating buffer (150 mM $NaHCO_3$ pH 9.6, 150 mM NaCl, 450 mL MQ water, 5 capsule HCO^-_3 (cat# C3041, Sigma). The plates were incubated for 1 h at RT and were washed 3x times in buffer (0.05% Tween-20/PBS w/o Ca^{2+} and Mg^{2+}). Ten µl/well of sulfo-tag solution (MSD Goat anti-human sulfo-tagged IgG (500 µg/ml) was added to each well and incubated for 30 min at RT. Subsequently, plates were washed 5x and 35 µl/well MSD Read Buffer with Surfactant (2x) and plates were analyzed by MSD instrument 600S. A Four Parameter Logistic (4PL) regression curve was fitted using Graphpad Prism 9.0 to determine EC50 of the antibodies. Each experiment was run in replicates and data normalized to background signal. Data depicted is calculated from three individual experiments.

To determine the binding affinity of α-syn antibodies to monomer α-syn, we performed kinetic analysis using surface plasmon resonance. The analysis was performed on a Biacore S200 system (Cytiva) using a capture kinetic set-up. The human α-syn antibodies were captured on a CM4 chip prepared by immobilization (amine coupling) of ~3000 RU of anti-human IgG antibody, following the protocol from Cytiva (BR1008-39 Cytiva). The α-syn antibodies were injected at 1 µg/ml with a contact time of 30 s to obtain capture levels of ~ 50–200 RU. HBS-P buffer (BR100671 Cytiva) with additives: 5 mg/ml BSA (A7979 Sigma Aldrich) and additional 0.05% P20 (total 0.1%) was used as running buffer and for sample dilution. Monomeric α-syn was used as analyte in a 3-fold dilution series from 0–300 nM or 0–600 nM. Regeneration of the capture surface was achieved by injection of 3 M $MgCl_2$ regeneration buffer, provided in the human antibody capture kit (BR1008-39 Cytiva). Data was analyzed using Biacore S200 Evaluation software. The K_D values and kinetic parameters were determination by global fit of sensorgrams to a 1:1 kinetics model.

The affinity of binding was also analyzed by Fluidigm to human α-syn monomer and oligomers (ND Biosciences).

Results

Generation and initial characterization of α-Synuclein antibodies

α-Syn specific antibodies were isolated from hybridomas from human antibody transgenic mice immunized with different combinations of recombinant α-syn fibrillar assemblies and truncated forms of monomeric α-syn. The primary selection of hundreds of hybridomas was done on an eight quadrant lay-out including human recombinant α-, β- and γ-synuclein, and the antibodies were selected based on binding selectively to α-syn. As a follow-up, antibodies were screened for preferred cross reactivity to cynomolgus, mouse and rat α-syn. Initial biolayer interferometry (BLI) binding data of representative purified antibodies Lu AF55696, Lu AF55699, Lu AF82422 and Lu AF55690 are listed in Fig. 1A. The linear epitopes of these four antibodies were assessed using peptide arrays scanning the entire α-syn sequence. Binding peptides for all the antibodies located to either the N- or C-terminal part of the protein and were outside of the central aggregating domain (NAC) based on published cryo-electron microscopy structures (indicated by L38-K97 multimers) (Fig. 1B)[64,65]. To ensure that the antibodies recognize disease-relevant forms of human α-syn, immunohistochemical staining's using Lu AF55696, Lu AF55699, Lu AF82422 and Lu AF55690 as primary detection antibody were performed on tissue sections of substantia nigra derived from two cases of PD positive for Lewy pathology. All antibodies clearly stained Lewy body-like structures within dopaminergic neurons (Fig. 1C).

Inhibition of seeded alpha-synuclein pathology and effect on seed cleavage in primary neurons

Seeding models, where intracellular α-syn aggregation is induced by the application of extracellular seeds, have been shown to recapitulate key aspects of LB and LN pathology[17] and are therefore ideal for evaluating the potential of α-syn antibodies to interfere with this process when applied extra-cellularly.

Therefore, we next assessed whether the α-syn antibodies could inhibit seeding of α-syn pathology in primary neurons using human recombinant α-syn seeds/assemblies. Cortical neurons derived from transgenic mice over-expressing human wildtype α-syn (F28 cultures) were seeded with α-syn assemblies of the P91 type and the resulting intracellular pathology load visualized by pS129 α-syn immune labeling. As shown in Fig. 2A, all antibodies dose-dependently inhibit seeding—with Lu AF82422 and Lu AF55699 being the most efficient. Isotype control Lu AF77829 did not have any effect on preventing seeding.

To assess the impact of α-syn antibodies on cellular handling of the seed material, cortical neurons from wildtype (wt) mice were co-treated with α-syn assemblies of the P91 type as seeds and saturating concentrations of the respective α-syn antibodies. In neurons only exposed to seeds and no antibodies, staining for human α-syn (visualizing the seeds, and not the endogenous mouse α-syn) after 24 h revealed that human seeds are taken up and part of the up-taken human α-syn seeds have been proteolytically cleaved into truncated α-syn species as seen on the western blot (WB) in Fig. 2B, "seed control" (part of full length human α-syn at 15 kDa reduced to an app. 12 kDa truncated protein). From the 24 h timepoint it also seems that the antibody Lu AF82422 compared to the other antibodies might reduce uptake of the seed. After 7 days in culture, most of the full length 15 kDa human α-syn arising from the added seed is gone, but interestingly the truncated 12 kDa species of α-syn remains in the cells treated with seeds and no antibodies (Fig. 2C, "seed control"). The 7 day timepoint also indicated that anti-α-syn antibodies affect proteolysis of the seed in different

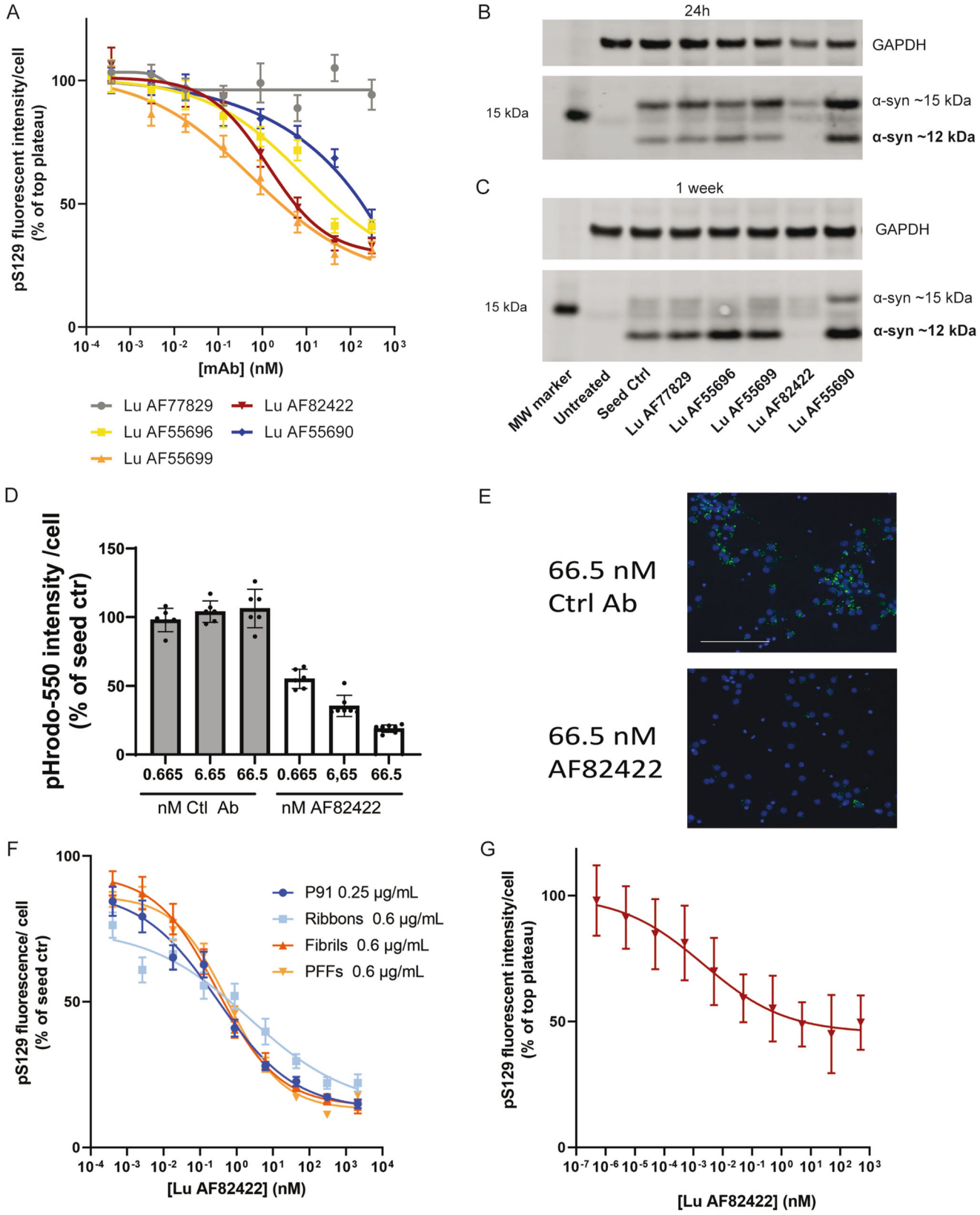

ways (Fig. 2B, C). Lu AF82422, with an epitope in α-syn including amino acids 112-117, prevents formation of truncated α-syn in the cells. In contrast, the other antibodies having epitopes in the N-terminal (Lu AF55696 (aa 1-15) and Lu AF55699 (aa 100-105)) or further C-terminally (Lu AF55690 (125-140)) do not prevent formation of truncated α-syn species arising from the added seeds. The isotype control Lu AF77829 did not have any effect on the formation of truncated α-syn seeds (Fig. 2C).

Based on the relative high seeding-inhibition efficiency combined with the ability to inhibit seed uptake and prevent the accumulation of truncated α-syn seed species, we decided to continue with a more extended profiling of Lu AF82422.

Fig. 2 | Antibodies inhibit seeded α-syn aggregation in mouse primary neuronal cells and affect uptake and truncations of seeds differently. A Antibody inhibition of seeding was examined in F28 primary mouse neurons with pS129 α-syn immunolabelling as a readout for seeding. Cells were treated at DIV5 with 0.4 μg/ml α-syn assemblies of the P91 type premixed with a dilution series of antibody and subsequently fixed and analyzed for pS129 immunolabelling and cell count after 7 days, $n = 4$ independent cultures. **B**, **C** Antibody effect on the uptake and proteolytic cleavage of full length human α-syn assemblies of the P91 type after 24 h and 1 week in wt mouse primary neuronal cultures. "Untreated" denotes naïve primary neurons while "Seed Ctrl" signifies primary neurons treated with full length human α-syn P91 but no antibody, $n = 2$ independent cultures. Full WB's are included in Supplementary Fig. 2A, B. **D** Lu AF82422 dose-dependent inhibits uptake of PFFs labeled with pHrodo. 0.5 μg/ml PFF-pHrodo premixed with a dilution series of Lu AF82422 added to F28 primary mouse neurons and fluorescence intensity per cell normalized to "seed only" quantified 48 h later, $n = 2–3$ independent experiments with $n = 2–3$ technical replicates each (=6–9 datapoints) cultures ± SD. **E** Representative images from 2D. Cells treated with either 66.5 nM control (Lu AF77829) or AF82422. Overlay of Hoechst in blue and PFF-pHrodo in green. Scale bar = 100 μm. **F** Lu AF82422 dose-dependently inhibits seeding induced by various recombinant α-syn assemblies (P91 0.25 μg/ml, Ribbons 0.6 μg/ml, Fibrils 0.6 μg/ml and PFF's 0.6 μg/ml) in F28 primary mouse neurons, $n > 3$ independent cultures ± SEM. **G** Lu AF82422 dose-dependently inhibits seeding induced by enriched MSA brain extract in F28 mouse primary neurons. Two different enriched MSA brain extracts originating from putamen were used, $n = 2$ independent cultures ± SD. Raw data from Cellomics quantifications reported in **A**, **F** and **G** are included in Supplementary File 2A–C. Full western blots of blots in **B** and **C** are included in Supplementary Fig. 2. Raw data from PFF uptake assays is included in Supplementary File 3.

Dose dependent seeding-inhibition with Lu AF82422 in F28 primary neurons was confirmed using a S129 α-syn FRET assay as an alternative quantitative readout for measuring α-syn aggregates (Supplementary Fig. 2C). Seeding inhibition with Lu AF82422 was also demonstrated in both wt and F28 primary neurons based on cellular fractionations into Triton soluble and Triton insoluble /SDS soluble fractions, followed by WB analysis (Supplementary Fig. 3). In these experiments both endogenous mouse α-syn and human α-syn is present in the Triton insoluble/SDS soluble fractions after seeding and Lu AF82422 clearly inhibits the formation of insoluble aggregated α-syn visualized by both a total α-syn-antibody or a pS129 α-syn antibody. Also, the experiments confirmed that Lu AF82422 prevents truncation of the original seed material.

To further investigate the mechanism by which Lu AF82422 prevent seeded aggregation, α-syn assemblies of the PFF type were labeled with the pH sensitive fluorophore pHrodo. As the environmental pH decreases during endocytosis of the seeds from pH ~6.3 in early endosomes towards pH ~4.7 in lysosomes, the pHrodo labeled seed will only be fluorescent in the lysosomes. Addition of PFF-pHrodo to F28 cortical neurons with increasing concentrations of Lu AF82422 demonstrated a dose-dependent reduction of fluorescence in lysosomes (Fig. 2D, E), indicating that Lu AF82422 inhibits uptake of the seeds. At the highest concentration of Lu AF82422 the seed uptake is reduced by ~80%.

To explore if Lu AF82422 can inhibit seeded aggregation induced by various α-syn assembly types reported to have different conformations, both P91, Ribbons, PFFs and Fibrils, were used to induce seeding. Lu AF82422 dose-dependently inhibit seeded α-syn aggregation irrespectively of the seed used (Fig. 2F). Finally, Lu AF82422 was shown to inhibit seeding in mouse primary neurons, induced by brain extract enriched from human MSA patient brains, in a dose dependent manner (Fig. 2G).

Lu AF82422 binds PD and MSA-derived aggregates similarly and stains LBs and GCIs in human brain tissue

The apparent binding affinity of Lu AF82422 to sarcosyl insoluble material isolated from PD and MSA patients' and healthy controls' brain tissues were determined by ELISA. Lu AF82422 showed both binding to MSA and PD fibrillar material and no binding to homogenates from healthy control brains Fig. 3A, B. The EC50 values deduced from the dose response shown are 0.09 nM for MSA and 0.16 nM for PD.

We verified that Lu AF82422 binds similarly to aggregated α-syn in brain tissue from PD, MSA and DLB patients by immunocytochemistry. In *Locus coeruleus* sections from PD patients, Lu AF82422 showed cytoplasmic labeling with a "fuzzy" border and labeled "corkscrew"-formed neurites, consistent with cytoplasmic LBs and LNs (Fig. 3C). Where the inclusions were singular, they have the morphological appearance of LBs (spherical and dense) (Fig. 3E). In cortical sections from DLB patients Lu AF82422 shows strong labelling of cortical LB-like inclusions (Fig. 3G). Other sections from the same study shows smaller neuritic pathologies (Supplementary Fig. 4). In cerebellum (Fig. 3D, H) and putamen (not shown) sections from MSA patients, Lu AF82422 shows extensive white matter pathology staining, in form of strong-positive GCIs characteristic of MSA.

To further characterize the binding of Lu AF82422 to α-syn, an immunoprecipitation (IP) was performed from MSA and healthy control tissue homogenates (putamen and cerebellum) followed by western blotting analysis of total and pS129 α-syn. The analysis confirmed efficient IP of α-syn with Lu AF82422, but not the control antibody (Fig. 4A, B). Binding to the full-length α-syn and its truncated forms was observed in putamen and cerebellum samples from MSA and healthy control. Notably, pS129 α-syn was only detected in homogenates from MSA material in line with high degree of aggregated α-syn in those samples and in support of the observed binding (Supplementary Fig. 5A). Similar results were obtained for Lu AF82422 binding to α-syn in PD and DLB brain homogenates (Fig. 4C). The amounts of pS129 α-syn bound in disease and control samples corresponded well with levels of α-syn aggregates measured in the untreated homogenates with an aggregation specific HTRF-based assay (Supplementary Fig. 5A).

To further support binding of Lu AF82422 to pathological α-syn present in MSA, PD and DLB material, a HTRF-based aggregation-specific analysis was performed on the immunodepleted homogenates to quantify the unbound aggregated α-syn (Fig. 4D). Representative brain homogenates carrying comparable pathology load were selected based on the initial analysis (Supplementary Fig. 5A) Diluted brain lysates were subjected to incubation with magnetic beads coated with Lu AF82422 or a control antibody. Lu AF82422 showed efficient depletion of α-syn aggregates comparing to the isotype control (Fig. 4D). Immunodepletion decreased the levels of α-syn aggregates detectable in disease material (MSA, PD and DLB) to the levels comparable to control brain homogenates indicating that Lu AF82422 can bind most of the pathological α-syn aggregates.

Crystal structure of Lu AF82422-α-syn complex reveals that affinity contributions are mainly driven by heavy chain CDRs binding to α-syn residues I112-L113 and D115-M116

The epitope of Lu AF82422 was mapped to the C-terminal residues 112-117 (ILEDMP) of α-syn using linear peptides by screening binding to an array of overlapping peptides (Fig. 1B). Lu AF82422 recognition of the epitope was further investigated and verified structurally by co-crystallization of a Lu AF82422 Fab fragment together with α-syn. This Fab-antigen complex was determined at 2.1 Å resolution by X-ray crystallography (Fig. 5A). Kabat numbering was applied to the antibody structure. The structure revealed the peptide in the binding pocket without any secondary structure elements. Quantification of the buried surface area between the α-syn epitope and Lu AF82422 yields 732 $Å^2$, with the majority engaged with the heavy chain (566 $Å^2$) compared to the light chain (242 $Å^2$). Consequently, only a few interactions are observed between the light chain of Lu AF82422 and the α-syn antigen. These include one hydrogen bond involving LC CDR3 Y91-OH and the main-chain carbonyl of G111; plus van der Waals contacts between LC CDR1 Y32-L113 and framework Y49 adjacent to LC CDR2

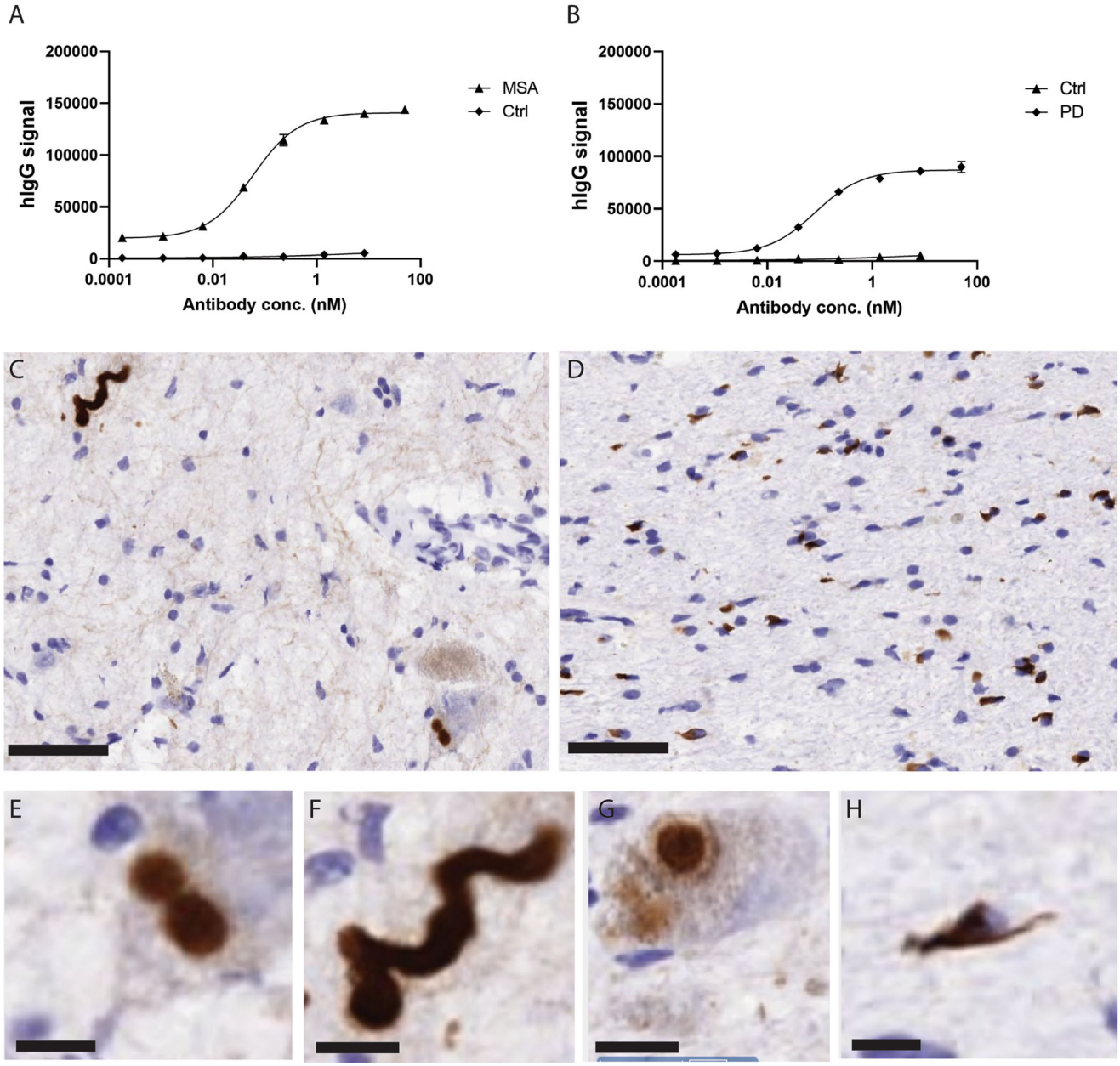

Fig. 3 | Lu AF82422 binds to pathological forms of α-syn in patient derived homogenates and brain sections. A, **B** ELISA measure of Lu AF82422 binding to α-syn aggregates derived from MSA and PD brains, respectively and compared to control brain. Lu AF82422 used for staining of **C** section from Locus coeruleus in PD patient showing corkscrew shaped neurite and cell with cytoplasmic Lewy bodies, **D** section from cerebellum in MSA patient showing extensive white matter pathology with multiple glial cytoplasmic inclusions. **E**, **F** Increased magnifications of Lewy bodies and Lewy Neurites from (**C**). **G** section from cortex in DLB patient showing a cytoplasmic Lewy body. **H** Glial cytoplasmic inclusion from (**D**). Scale bar = 50 nm in (**C**, **D**), 10 nm in (**E**–**H**).

with I112. In contrast, Lu AF82422 establishes eight hydrogen bonds with α-syn through main chain and side chain residues of all three HC CDRs. Multiple hydrophobic contacts are observed, e.g. HC CDR3 W96 gets sandwiched between the side chains of L113 and M116. The side chain of the latter fits into a cavity created by residues A33, R52, and W96 presented by the three different HC CDRs. The well resolved peptide allowed for assessment of binding contributions by free-energy perturbation through in silico alanine scanning (Fig. 5B, C). In good agreement with the epitope mapping, in silico substitutions of I112A, L113A, D115A and M116A considerably decrease ΔΔG binding by more than 3 kcal/mol, while residues E114A and P117A each contributes a predicted ΔΔG lowered by 1 kcal/mol.

In vivo inhibition of seeding by Lu AF82422

To complement our in vitro data, the ability of Lu AF82422 to inhibit seeded α-syn aggregation in vivo was investigated. α-Syn assemblies of the Fibrillar type (molar concentration of fibrils was based on the monomer concentration prior to fibrillation and was fixed at 133 μM, corresponding to 2 μg fibrils) were pre-mixed with Lu AF82422 or a control hIgG (Lu AF77829). Lu AF77829 was mixed with Fibrils in a molar ratio antibody:Fibrils of 1:1. Lu AF82422 was mixed with Fibrils at a molar ratio antibody:Fibrils of 1:1, 1:3 or 1:10. Six weeks following unilateral intra-striatal injection of the antibody-fibril mix, the number of pS129-α-syn positive neurons in the substantia nigra ipsilateral to the injection site was quantified (Fig. 6). Compared to the control

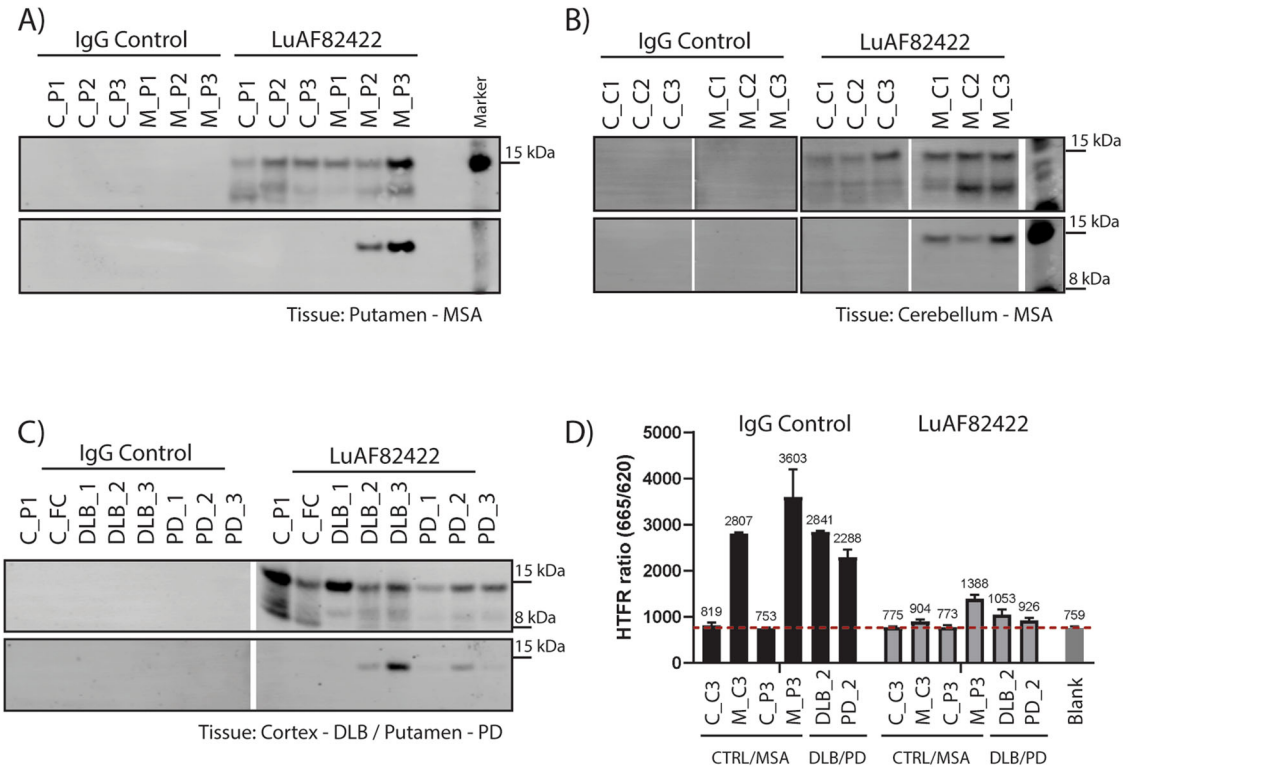

Fig. 4 | Immunoprecipitation and immunodepletion of α-syn from MSA, PD and DLB brain tissue material. WB analysis of α-syn IP'ed with Lu AF82422 from MSA brain homogenates, putamen (**A**) and cerebellum (**B**), and corresponding controls. α-Syn is visualized using total or pS129-α-syn antibodies. **C** IP and western blotting analysis performed as in (**A**) but using PD (putamen) and DLB (cortex) brain homogenates, and matching controls. **D** HTRF-based analysis of α-syn aggregates in brain homogenates immunodepleted with Lu AF82422 or control antibody. Samples were selected to represent similar pathology load (Supplementary Fig. 5A). HTRF ratio is plotted as measure of aggregated α-syn over experimental background. See Supplementary Table 1 for additional information on tissue samples. Full western blots of **A**–**C** and raw data for the HTFR assay are included in Supplementary Fig. 5B–D and Supplementary File 5, respectively.

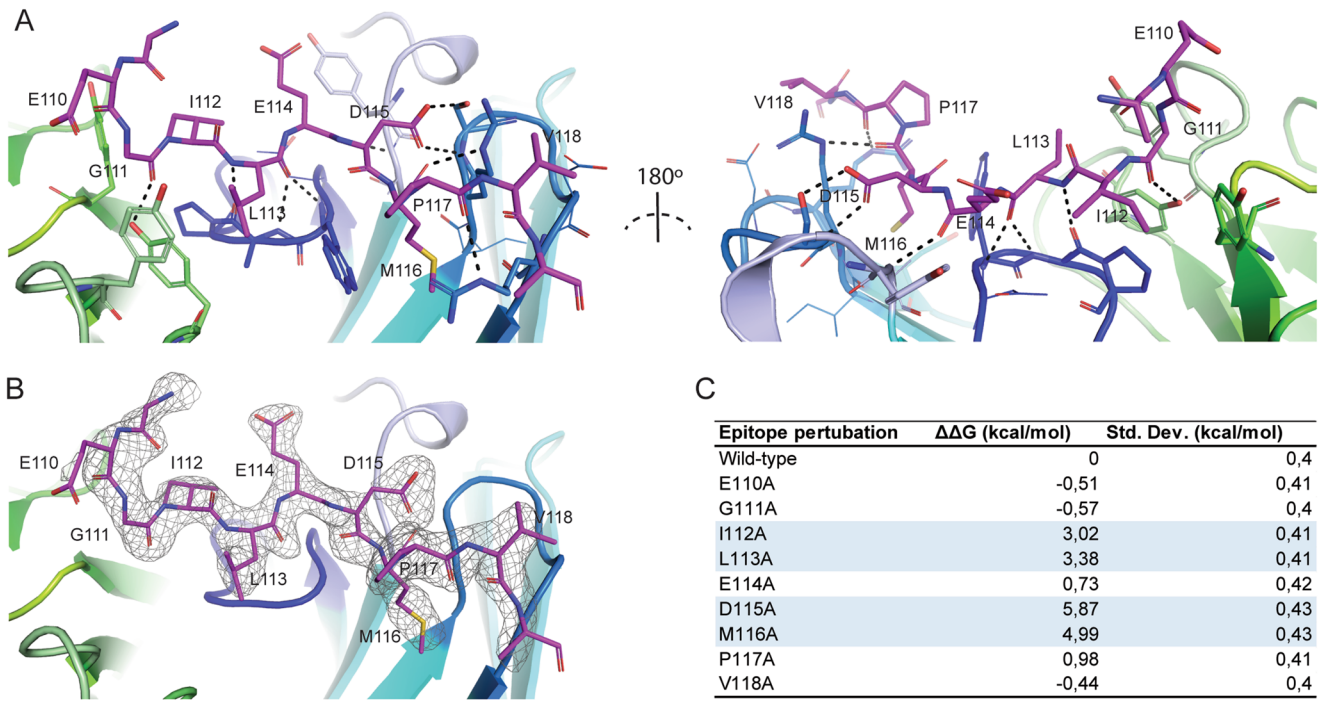

Epitope pertubation	ΔΔG (kcal/mol)	Std. Dev. (kcal/mol)
Wild-type	0	0,4
E110A	-0,51	0,41
G111A	-0,57	0,4
I112A	3,02	0,41
L113A	3,38	0,41
E114A	0,73	0,42
D115A	5,87	0,43
M116A	4,99	0,43
P117A	0,98	0,41
V118A	-0,44	0,4

Fig. 5 | Crystal structure of Lu AF82422 binding to α-syn. A Crystal structure of the Lu AF82422:α-syn complex rotated 180°. Light chain of Lu AF82422 shown in green, heavy chain in blue and α-syn in red. Key residues are shown as sticks and hydrogen bonds as dashes (black). **B** Difference electron density (mFo-DFc) of the epitope peptide indicates that it is well resolved in the binding pocket. **C** In silico free energy perturbation by alanine scanning through the epitope based on the crystal structure. Key affinity driving residues with contributions to ΔΔG > 1 kcal/mol are highlighted (blue).

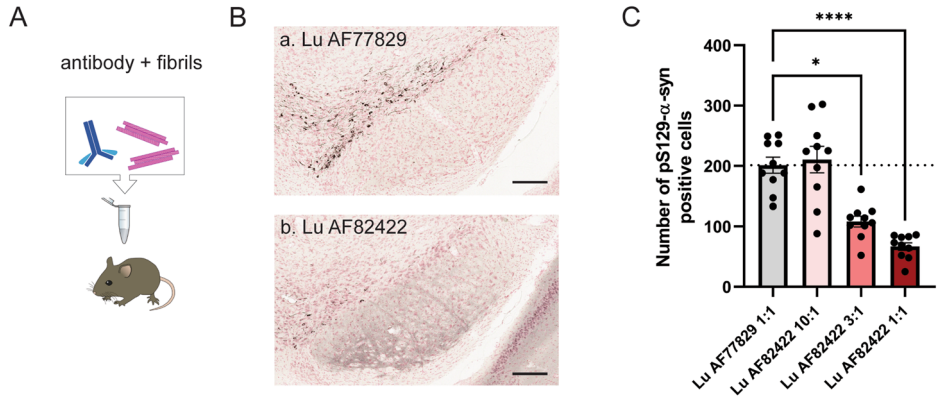

Fig. 6 | Lu AF82422 dose-dependently inhibits seeding in a co-injection paradigm in mice. **A** Antibodies and α-syn assemblies of the Fibrillar type were pre-mixed prior to intrastriatal injection; for each injection, 2 µg of Fibrils were mixed with varying amounts of antibodies, at Fibril:antibody monomer molar ratio of 1:1, 3:1 or 10:1. **B** Representative images depicting pS129-α-syn positive staining in the substantia nigra of animals injected with Fibrils mixed with Lu AF77829 (control hIgG) or Lu AF82422 at 1:1 ratio; scale bar: 100 µm. **C** The number of pS129-α-syn positive cell bodies was quantified in animals injected with Fibrils mixed with Lu AF82422 at 1:1, 3:1 or 10:1 and compared to the numbers from animals injected with Fibrils mixed with Lu AF77829 at 1:1. Data were analyzed by a one-way ANOVA followed by Kruskal–Wallis post hoc comparison.

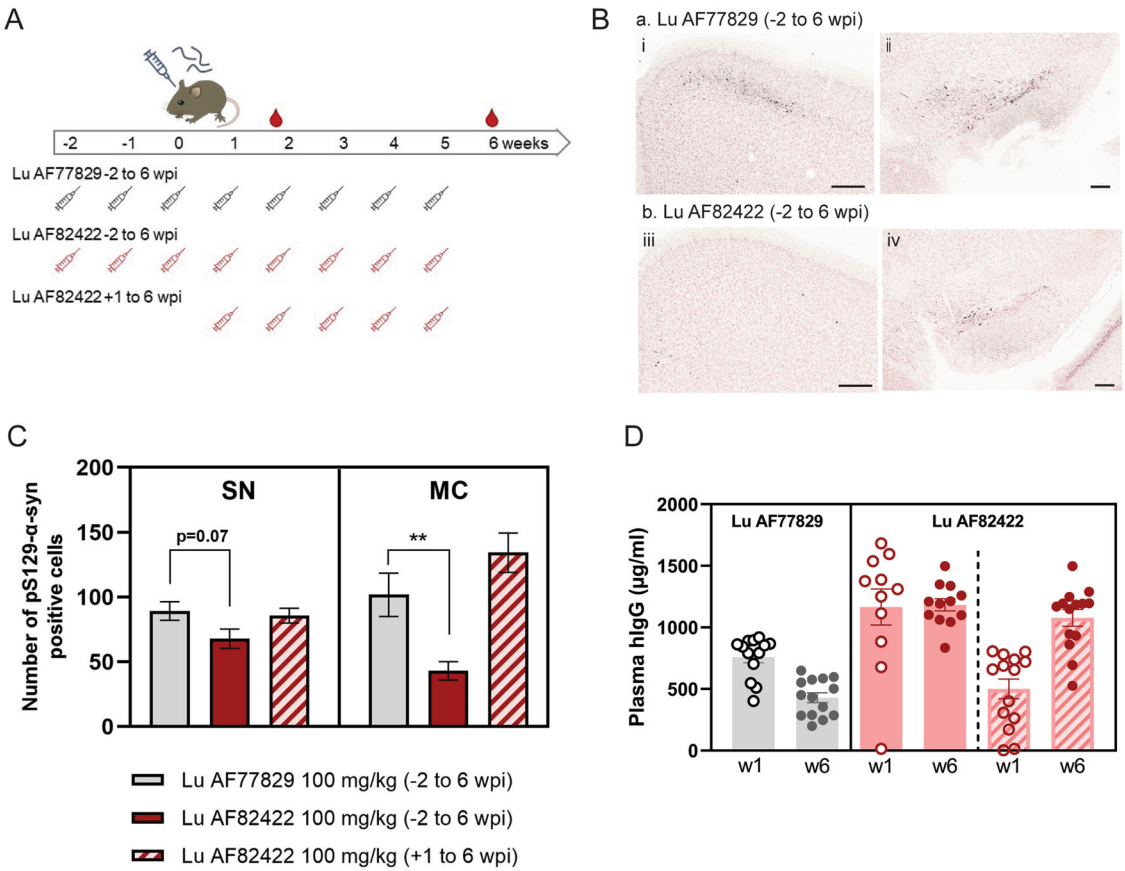

Fig. 7 | Lu AF82422 inhibit seeding following systemic dosing in mice. **A** Mice were assigned to three different treatment groups: Control hIgG, Lu AF77829 administered once weekly (100 mg/kg i.p.) from 2 weeks before and up to 6 weeks after seeding initiation (−2 to 6 weeks post-injection, −2 to 6 wpi); Lu AF82422 administered once weekly (100 mg/kg i.p.) from 2 weeks before and up to 6 weeks after seeding initiation (−2 to 6 wpi); Lu AF82422 administered once weekly (100 mg/kg i.p.) from 1 weeks after and up to 6 weeks after seeding initiation (+1 to 6 wpi). All mice were injected intrastriatally with α-syn assemblies of the P91 type and sacrificed 7 days after the last administration of antibody. A blood sample was collected at the end of week 1, as well as terminally, 7 days after the last administration of antibody. **B** Representative images depicting pS129-α-syn positive staining in the motor cortex (MC; i, iii) and substantia nigra (SN; ii, iv) of animals injected with P91 and treated weekly with Lu AF77829 (a) or Lu AF82422 (b) from −2 to 6 wpi. Scale bar: 100 µm. **C** Number of pS129-α-syn positive cell bodies quantified in the substantia nigra (SN) and motor cortex (MC) indicate a reduction in pathology load in animals treated with Lu AF82422 from −2 to 6 wpi. Data were analyzed by a one-way ANOVA followed by Holm-Sidak's post-hoc comparison. **D** Plasma hIgG levels measured by LC-MS at the end of week 1 and week 6.

antibody Lu AF82422 significantly and concentration-dependently reduced the pS129-α-syn pathology in the *substantia nigra*.

To further consolidate these in vivo data, the ability of Lu AF82422 to prevent seeded aggregation following systemic administration was evaluated. For these studies α-syn assemblies of the P91 type was used. As these assemblies are more potent it allowed for an 8-fold reduction in seed concentration (corresponding to 0.25 µg). Compared to published studies[18,63] typically using seed amounts of approximately 4 to 5 µg per injection site, we do recapitulate a similar regional distribution of the spreading of pathology, including motor cortex, amygdala and

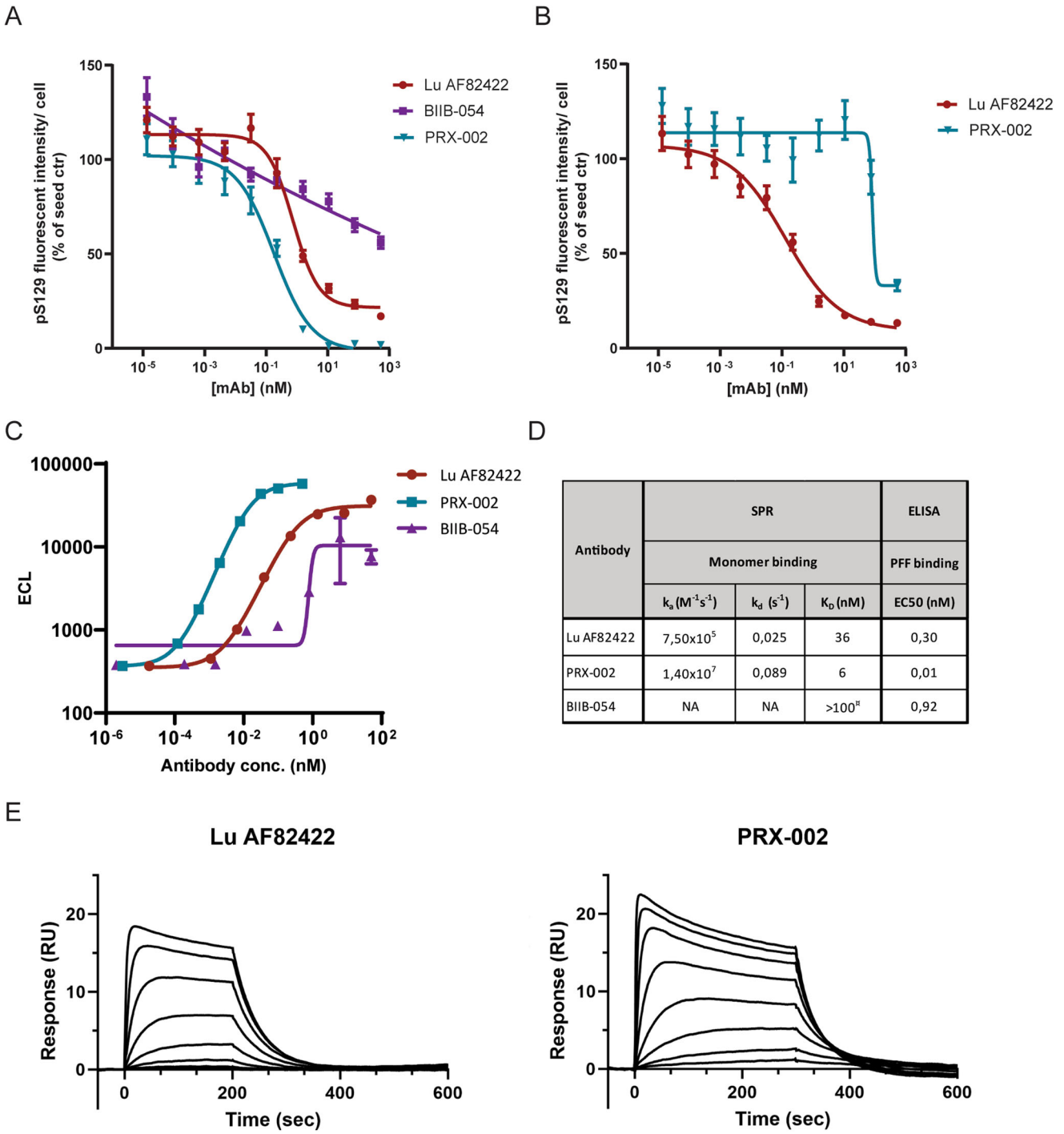

Antibody	SPR			ELISA
	Monomer binding			PFF binding
	k_a ($M^{-1}s^{-1}$)	k_d (s^{-1})	K_D (nM)	EC50 (nM)
Lu AF82422	7,50x10^5	0,025	36	0,30
PRX-002	1,40x10^7	0,089	6	0,01
BIIB-054	NA	NA	>100[#]	0,92

Fig. 8 | Side-by-side comparison of Lu AF82422, cinpanemab and prasinezumab in primary neuron α-syn seeding assay. A Antibody inhibition of seeding with Lu AF82422, cinpanemab and prasinezumab in F28 primary neurons. Cells were treated at DIV5 with 0.5 ug/mL α-syn assemblies of the PFF type premixed with dilution series of antibody and analyzed for pS129 immunolabelling and cell count after 7 days, $n = 4$ independent cultures ± SEM. **B** Lu AF82422 effectively inhibits seeding of truncated α-syn (1-119) in F28 primary neurons but prasinezumab does not. Cells were treated with 0.4 µg/mL 1-119 truncated α-syn assemblies of the PFF type premixed with dilution series of antibody and analyzed for pS129 immunolabelling and cell count after 7 days, $n = 3$ independent cultures ± SEM. **C** Binding of Lu AF82422, prasinezumab and cinpanemab to α-syn assemblies of the PFF type in ELISA. **D** k_a, k_d and K_D for Lu AF82422, cinpanemab and prasinezumab binding to monomeric alpha-synuclein determined by SPR, as well as EC50 values for binding to PFF determined by ELISA. Poor SPR kinetics observed for cinpanemab. NA non-applicable. **E** Representative SPR sensorgram of Lu AF82422 and PRX-022 binding to monomeric α-syn using 0–600 nM and 0–300 nM dilution series. Raw data from Cellomics quantifications reported in **A** and **B** are reported in Supplementary File 6.

substantia nigra, although the amount of pathology is milder than in the studies mentioned above (Supplementary Fig. 6). Mice were dosed weekly at 100 mg/kg i.p. for a control and Lu AF82422 group starting 2 weeks prior to seeding. In addition, for one group of mice Lu AF82422 treatment was initiated 1-week post-challenge (Fig. 7A). Compared to the control antibody Lu AF82422 reduced the pS129-α-syn pathology in the substantia nigra and significantly in motor cortex ipsilateral to the injection site when weekly dosing was initiated prior to seed injection, but not if dosing started after seeding (Fig. 7B, C).

Human IgG levels were quantified in plasma 1 week after seeding initiation, and terminally at week 6 (Fig. 7D). Mice treated with Lu AF82422 from 2 weeks prior to seeding showed stable plasma levels at week 1 after seeding (1166 ± 146 ug/ml) and at week 6 (1183 ± 50 ug/ml), while mice that initiated treatment with Lu AF82422 1 week after seeding exhibited lower initial levels (501 ± 80 ug/ml) as expected but increased up to comparable levels (1077 ± 68 ug/ml) at week 6 as the animals treated from 2 weeks prior to seeding.

In vitro functional comparison of Lu AF82422 to cinpanemab and prasinezumab

To increase the understanding of similarities and differences between Lu AF82422 and the two α-syn antibodies, prasinezumab and cinpanemab, previously or currently in clinical development in PD, we compared the three antibodies side-by-side in the assay of seeded α-syn pathology development in primary neurons. Cinpanemab showed relative low potency in inhibition of α-syn pathology development in F28 primary neurons whereas prasinezumab, similarly to Lu AF82422, potently inhibited seeding induced by α-syn assemblies of the PFF type as seeds (Fig. 8A). Because of the association of CTT α-syn with disease we further evaluated the ability of prasinezumab and Lu AF82422 to prevent α-syn pathology development if the seeding was induced by assemblies of the PFF type made from truncated human α-syn 1-119. Under these conditions Lu AF82422 potently inhibited seeding whereas prasinezumab only showed a moderate effect with inhibition at the highest dose (Fig. 8B). Follow-up assessment of the binding affinity of Lu AF82422 showed comparable binding to truncated aa 1-119 and full length α-syn (data not shown).

The EC50 values for Lu AF82422 binding to fibrillar α-syn was determined by an ELISA with fibrillar α-syn assemblies of the PFF type coated plates to be 0.30 nM (Fig. 8C). The binding affinity (K_D) for Lu AF82422 binding to recombinant human monomeric α-syn was determined by SPR to be 36 nM (Fig. 8D, E). The published binding characteristics of both prasinezumab[66] and cinpanemab[67] to fibrillar α-syn (0.01 nM and 0.92 nM, respectively) (Fig. 8C, D) and to α-syn monomer (K_D 6 nM and based on poor kinetics >100 nM, respectively) (Fig. 8D, E) were confirmed by the same methods.

As a more explorative approach the binding affinities to α-syn were also analyzed by microfluidic diffusional sizing (MDS) on oligomers from ND Biosciences[68]. The interactions were investigated by monitoring changes in the diffusion coefficients of the equilibrated species through MDS, a method used previously to evaluate binding of antibodies to Abeta oligomers[69]. Using this method, the binding affinities for Lu AF82422 to monomers and oligomers was determined to be 12 nM and 0.3 nM respectively.

Discussion

Passive immunotherapy with the aim of inhibiting propagation of pathology in α-synucleinopathies is an active field of drug development in PD and MSA. Several mechanisms by which α-syn antibodies could interfere with progression of pathology have been proposed based on studies in preclinical models (reviewed in ref. 38). These include extracellular binding to pathological α-syn seeds and therefore inhibition of direct toxicity, inhibition of neuronal/oligodendrocyte uptake of seeds and/or facilitated microglial mediated clearance of seeds. It is not yet clear which of these mechanisms will be most important to drive efficacy in patients.

In prioritizing Lu AF82422 over other antibodies from the campaign we focused on functional effects in assays of seeded aggregation as well as inhibition of seed uptake and prevention of proteolytic cleavage/intracellular accumulation of α-syn seeds. The seeding models, in contrary to models of transgenic overexpression of α-syn, capture relevant aspects of intracellular α-syn pathology[70] and due to the extracellular component in the models, e.g., the exogenous α-syn seeds, they allow for functional evaluation of antibodies in an experimental set-up approximating the prion-like hypothesis of pathology spread in patients with α-synucleinopathies.

An important limitation both in vitro and in vivo using these models are the non-physiological high concentrations of seeds, and therefore antibody, required for achieving meaningful assay windows. To strengthen the rationale for a therapeutic effect of Lu AF82422 we therefore investigated the effect of systemic administration of the antibody. By using a more potent fibrillar α-syn assembly the seed concentration required could be reduced by 8-fold. In this model we demonstrated significant robust reduction (50–60%) of α-syn pathology development in motor cortex and a tendency for reduction in substantia nigra *pars compacta* if Lu AF82422 was predosed for 2 weeks prior to seed injection (Fig. 7C). The reason for the observed regional differences could be related to our observation that pathology in the motor cortex develops first following intra-striatal seed injection, even before any PS129α-syn positive cells are present in the substantia nigra *pars compacta*. There could be several factors underlying this: for example the distance of the cell bodies to the injection site (the shorter distance the faster pathology development), the higher PS129α-syn levels in cortical regions under physiological conditions[71] but also the level of neuronal activity in corticostriatal vs. nigrostriatal projections[72,73]. It is also clear that pre-dosing of Lu AF82422 prior to seed injection provides the most optimal scenario for obtaining an efficacy readout. In this scenario the exposure of the antibody has reached steady state and is present in high amounts able to immediately bind the injected seeds. No inhibition of pathology development was observed, when Lu AF82422 treatment was initiated 1 week after seed injection. Seed uptake occurs rapidly within 24–48 h (Fig. 2B, D) and if the antibody is not present at the time when the seeds are available for binding in the extracellular space it will not be able to inhibit the seeded aggregation. Similar observations have been published in hippocampal slice cultures, where addition of an α-syn antibody was able to inhibit seeded α-syn aggregation in a pre-treatment paradigm but not when added 1 h after seed exposure[74]. Importantly, the implications of these findings are that whereas α-syn targeting antibodies have the potential to slow further disease progression by inhibiting further pathology development, they will have no impact on already established pathology. In a similar in vivo model, we have observed a marginal loss of TH positive cells in the substantia nigra of approximately 10% after 6 months (data not shown). The limited window, variability between animals, combined with a long dosing regimen precluded our ability to investigate the effect of Lu AF82422 on preventing cell death. Several groups have however reported a correlation between pS129 pathology and neuronal degeneration[75], and we hypothesize that Lu AF 82422 may prevent neurodegeneration because of the prevention of pS129- α-syn pathology development.

Our data points towards inhibition of seed uptake as the primary mechanism by which Lu AF82422 inhibit seeded aggregation (Fig. 2D). Interestingly even in the presence of the highest concentration of antibodies there is always a smaller fraction (~ 20%) of the added seeds that are taken up by the neurons (Fig. 2B, D). In the neurons the seeds are rapidly truncated to a 12 kDa α-syn species, and within 1 week, only the 12 kDa species is present (compare Fig. 2B, 24 h to 2C, 1 week). It is well characterized that α-syn is susceptible to proteolysis, and both N- and C-terminal truncations have been reported in human brain. The most common proteolysis site in human brain is amino acid 119[32,76]. Especially the C-terminal truncated forms have been shown to potentiate the propensity of α-syn to pathologically misfold into uniquely toxic fibrils with modulated prion-like seeding activity[76]. Truncations of α-syn have also been reported increased in MSA brain compared to control and PD brain[34]. This might point to a different processing of α-syn in MSA. Recently it was reported that α-syn truncated at residues 103, 115, 119, and 125 was readily present in MSA oligodendroglia cytoplasmic inclusions, but 122 cleaved α-syn was only weakly or not present. Conversely, MSA neuronal pathology in the pontine nuclei was strongly reactive to the α-syn x-122 neo-epitope but did not display any reactivity for α-syn 103 cleavage[77].

In the cells treated with Lu AF82422 α-syn truncation is not observed, resulting in no overall accumulation of the added human α-syn seeds. None of the other α-syn antibodies evaluated were able to prevent this accumulation of truncated seed material (Fig. 2C). We hypothesize that the epitope

of the antibodies can be an explanation for this difference. Lu AF8244 with an epitope on α-syn from aa 112-117 will be able to sterically hinder cleavage of the full length α-syn around aa 119-122 into the observed 12 kDa fragment, whereas the epitope of Lu AF55696 (α-syn 1-15), Lu AF55699 (α-syn 100-105) and Lu AF55690 (α-syn 126-140) (Fig. 1B) will not. Given the aforementioned literature on an increased presence of truncated α-syn in PD and MSA brain[34] with increased toxicity[76] we consider the unique feature of Lu AF82422 to be favorable.

As the precise nature of the pathological species of α-syn in various α-synucleinopathies is not known we rationalized that confirming both binding to and functional inhibition of as many forms of pathological α-syn as possible would increase the strength of Lu AF82422 as a potential therapeutic antibody. We demonstrate binding of Lu AF82422 to α-syn pathological inclusions/species in PD, MSA and DLB by both histology (Figs. 1C and 3C–H) and immunoprecipitation (Fig. 4A–C). In the immunoprecipitations we further demonstrate that Lu AF82422 can deplete aggregated α-syn forms from both MSA, DLB and PD human brain homogenates (Fig. 4D). We also confirmed direct binding of Lu AF82422 to α-syn in brain homogenates derived from MSA and PD patients (Fig. 3A, B). Importantly, the functional impact of binding to various pathological forms of α-syn aggregates was demonstrated by the ability of Lu AF82422 to dose-dependently inhibit seeding in primary mouse cultures regardless of the seed used (Fig. 2F, G).

To support investigations of cross species target engagement and preclinical toxicology studies we investigated the epitope of Lu AF82422 structurally by X-ray crystallography. The overall amino acid homology of α-syn between human and rodent is 95% and 99% between human and cynomolgus monkey. The 6 amino acids (I_{112}LEDMP$_{117}$) in the binding epitope for Lu AF82422 is identical in human and mouse, hence same affinity is expected. However, in cynomolgus monkey, position 114 is glutamine (Q114) while this is glutamate in humans (E114). The crystal structure reveals the side chain of E114 pointing away from the binding pocket and hence its contribution to binding is limited. This is confirmed by the low ΔΔG determined for E114 in FEP analysis (Fig. 5C), thus supporting a likely full cross-reactivity to cynomolgus monkey α-syn. The target engagement of Lu AF82422 on α-syn monomer in plasma and CSF as well as pre-clinical toxicology assessments in cynomolgus monkey has been reported separately[44].

One major challenge with immune based therapies in the brain is to overcome the blood brain barrier and secure high enough brain exposure to support target engagement. The reported exposure levels of antibodies in CSF are usually 0.1–0.4% of the serum levels[78] and we measure 0.22–0.29% in CSF with Lu AF82422 in cynomolgus monkey and 0.16% to 0.51% in humans[44,79]. In the seeding model we dosed 100 mg/kg of Lu AF82422 resulting in a steady state plasma concentration of around 1100 µg/mL (7.6 µM) (Fig. 7D), corresponding to a CSF concentration in the low nM range. According to the prion-like hypothesis, we assume that the pathological α-syn form is oligomeric or fibrillar, which means that the binding affinity to these species is the important factor. As assays for quantification of fibrillar α-syn in CSF is not available to support direct target engagement, the target engagement based on binding to monomeric α-syn can be used as a proxy in combination with the direct measurements of K_D to monomeric and fibrillar α-syn. This approach has been applied to other α-syn targeting antibodies in the clinic[80,81]. Affinities corresponding to 36 nM and 0.3 nM of Lu AF82422 to monomeric and fibrillar α-syn, respectively (Fig. 8D) would allow for target engagement of up to 20% on monomer and 90% on fibrillar α-syn in CSF at antibody doses resulting in plasma levels of 7.6 µM. This is similar to what was measured at the highest dose in the single ascending dose study for Lu AF82422[79].

A limitation with the in vivo seeding model in supporting the prediction of clinical doses is that it cannot be ruled out that the blood brain barrier breach during injection of the seeds is contributing to an additional influx of antibody to the brain and thereby resulting in an underestimation of the dose needed to inhibit seeding. A further refinement of the seeding model where the effect of peripheral dosed antibody could be investigated on secondary seeding in areas not directly connected to the injection site would be optimal. Development of a model recapitulating cell-to-cell transmission of aggregates is supported by literature[82,83], but they require dosing of the antibody for 2–3 months (the time between primary and secondary seeding) and might not be compatible with dosing a human antibody in mouse due to the high likelihood of raising an immune response against the human antibody.

α-Syn antibodies in clinical trials in α-synucleinopathies have been reviewed recently[84]; two of them have been in phase 2 studies in PD patients. The phase 2 PASADENA study on prasinezumab, although not showing significant difference from placebo in the sum of scores on parts I, II, and III of the MDS-UPDRS, did have numeric difference in part III (reflecting the motor assessment) and in a digital motor assessment[41]. prasinezumab is now in a phase 2b study in PD where the motor progression is the primary endpoint. The cinpanemab phase 2 clinical study in PD did not show significant difference from placebo in clinical measures of disease progression[42], and did not show any significant difference from placebo in the part III motor score. Biogen has reported that the project has been discontinued.

To understand the future potential of α-syn immunotherapy in PD and other α-synucleinopathies it is important to discuss learnings on similarities and differences of the antibodies being pursued. Two things will be important to know before any general conclusions can be made on whether immunotherapy targeting α-syn is promising or not. The first is data on brain exposure of the potential therapeutic antibody and the assessment of target engagement. The second important aspect is the mechanism by which the antibodies exert their functional effect.

The half-life of the antibody together with dose, dosing frequency and tissue binding are important factors for the availability to engage with the target in the brain. The reported T½ of prasinezumab is 10–18 days[66] compared to the T½ = 28 to 35 days of cinpanemab[85] and T½ = 28–30 days of Lu AF82422[79]. In phase 2 studies both prasinezumab and cinpanemab were dosed every 4 weeks with highest doses being 4500 mg and 3500 mg respectively[40,42]. Data on non-specific tissue binding or other attempts to assess unspecific binding has not been reported on other α-syn antibodies. In the histological staining's using Lu AF82422 reported here we did not see any evidence for unspecific staining in alignment with safety assessments and PK published on Lu A82422[44].

So far, target engagement data has not been reported from the two phase 2 clinical studies on prasinezumab[41] and cinpanemab[42]. The same calculations as applied above on Lu AF82422 was originally published on prasinezumab[66] and as such it should be possible to calculate a theoretical target engagement on fibrillar α-syn based on measured target engagement on α-syn monomer in the phase 2 study. This method can however not be applied to cinpanemab, because the binding affinity to α-syn monomer for this antibody is very low. The whole field would strongly benefit from highly sensitive and robust assays that can quantify fibrillar α-syn directly. Several promising assays has been published, especially assays based on seed amplification such as Real-time Quaking Induced Conversion (RT-QuIC) or Protein Misfolding Cyclic Amplification (PMCA)[86]. These assays exploit the intrinsic ability of misfolded α-syn to induce misfolding and aggregation of monomeric α-syn, which can then be monitored by the amyloid sensitive fluorophore thioflavin T. While these assays are currently not quantitative, they show great potential in early diagnostics as well as in stratification of α-synucleinopathies[87]. Furthermore, they may be combined with other markers, such as neurofilament light (NfL), to further refine usage as tool for biomarker analysis[88]. Attempts to make them quantitative are ongoing, e.g., by combining amplification with oligomer ELISA assay[89] and it will be very interesting to see these matured and applied in clinical trials.

As mentioned above several mechanisms of how α-syn antibodies can interfere with disease progression has been proposed. Prasinezumab and cinpanemab were selected based on different criteria for binding to α-syn and based on different preclinical models, either transgenic[37] or seeding models[67], but they have not been compared side-by-side in the same model(s). As the seeding models have been central in the selection of Lu AF82422 we found it relevant to compare the three antibodies side-by-side in the primary neuron seeding assay. To do this, we produced prasinezumab

and cinpanemab based on CAS register sequences and verified the binding of the antibodies to monomeric and fibrillar α-syn. The binding of prasinezumab to fibrillar α-syn was 0.01 nM corresponding well to the published data; 0.048 nM[66] and the binding of cinpanemab to fibrillar α-syn was 0.92 nM, also corresponding well to original published data[67] (and lower than recently independently published data; 9.5 nM[90]).

The data in the seeding model show that prasinezumab, as Lu AF82422 dose-dependently inhibit seeded aggregation, whereas cinpanemab was much less potent (Fig. 8A). The epitope of cinpanemab is in the N-terminal of α-syn (aa 1-10)[67] compared to the more C-terminal epitopes of prasinezumab (aa 118-126)[37] and Lu AF82422 (aa 112-117). Our data do not indicate that it is the epitope that determine an effect in this assay, as one of the other antibodies from our campaign Lu AF55696 also have an N-terminal epitope (aa 1-15) and dose-dependently inhibit seeded aggregation in the same assay (Fig. 2A).

As both prasinezumab and Lu AF82422 have epitopes around one of the major truncation sites in α-syn[76], we evaluated the ability to inhibit seeded aggregation induced by a truncated seed (seeds produced from α-syn aa 1-119). Here Lu AF82422 dose-dependently inhibited seeding and prasinezumab had some effect at the highest dose (Fig. 8B). If truncated forms of α-syn play a role in the pathology, as has been suggested by increased amounts of truncated species in pathological inclusions in diseased human brain[34,91], antibodies binding to more central epitopes would have an advantage.

Overall, based on our data, we hypothesize that the main driver of efficacy of α-syn targeting antibodies in the models of seeded aggregation is the binding to pathological α-syn seeds in the extracellular space, which prevents internalization of most of the seed material by neurons and/or oligodendrocytes. As some smaller seeds and/or seed/antibodies-complexes are taken up by neurons, we also propose that antibodies able to facilitate neuronal degradation of the seed material will have an added benefit in the brain, because truncated seeds, either released or in the cells, will be potent drivers of further pathology spreading.

In summary, we have developed a human antibody which can bind most α-syn species, including various fibrillated assemblies, as well as phosphorylated and truncated forms derived from human brain. Importantly Lu AF82422 can functionally inhibit seeded aggregation of α-syn, including seeding induced by truncated α-syn seeds and material directly enriched from MSA brains. The main mechanism by which Lu AF82422 inhibits seeded aggregation is prevention of seed uptake. It also results in no accumulation of the smaller fraction of seeds that are internalized.

Lu AF82422 has been in a phase 2 study in MSA (Trial identifier NCT05104476) and although primary endpoint was not met, there was a trend of a slowing MSA progression in the group exposed to Lu AF82422. Overall, the further development of Lu AF82422 will bring valuable contributions to our understanding of the potential of α-syn immunotherapies in the treatment of α-synucleinopathies in the years to come.

Data availability

The crystal structure of Lu AF82422 in complex with α-syn is available from the Protein Data Bank repository. PDB ID: 8B9V. The sequence for Lu AF82422 is available in the CAS register (2850367-41-6). All other data are presented in full within this paper.

Received: 31 May 2024; Accepted: 28 November 2024;
Published online: 22 May 2025

References

1. Papp, M. I. & Lantos, P. L. The distribution of oligodendroglial inclusions in multiple system atrophy and its relevance to clinical symptomatology. *Brain J. Neurol.* **117**, 235–243 (1994).
2. Papp, M. I. & Lantos, P. L. Accumulation of tubular structures in oligodendroglial and neuronal cells as the basic alteration in multiple system atrophy. *J. Neurol. Sci.* **107**, 172–182 (1992).
3. Engelhardt, E. Lafora and Trétiakoff: the naming of the inclusion bodies discovered by Lewy. *Arq. Neuropsiquiatr.* **75**, 751–753 (2017).
4. Lewy, F. H. in *Handbuch der Neurologie,* Vol. 3 (ed. Lewandowsky, M.) Ch. I. Pathologische Anatomie, 920–958 (Springer, 1912).
5. Papp, M. I., Kahn, J. E. & Lantos, P. L. Glial cytoplasmic inclusions in the CNS of patients with multiple system atrophy (striatonigral degeneration, olivopontocerebellar atrophy and Shy-Drager syndrome). *J. Neurol. Sci.* **94**, 79–100 (1989).
6. Spillantini, M. G. et al. Filamentous alpha-synuclein inclusions link multiple system atrophy with Parkinson's disease and dementia with Lewy bodies. *Neurosci. Lett.* **251**, 205–208 (1998).
7. Wakabayashi, K. et al. Accumulation of alpha-synuclein/NACP is a cytopathological feature common to Lewy body disease and multiple system atrophy. *Acta Neuropathol.* **96**, 445–452 (1998).
8. Braak, H. et al. Staging of brain pathology related to sporadic Parkinson's disease. *Neurobiol. Aging* **24**, 197–211 (2003).
9. Borghammer, P. et al. Neuropathological evidence of body-first vs. brain-first Lewy body disease. *Neurobiol. Dis.* **161**, 105557 (2021).
10. Brettschneider, J. et al. Converging patterns of alpha-synuclein pathology in multiple system atrophy. *J. Neuropathol. Exp. Neurol.* **77**, 1005–1016 (2018).
11. Li, J. Y. et al. Lewy bodies in grafted neurons in subjects with Parkinson's disease suggest host-to-graft disease propagation. *Nat. Med.* **14**, 501–503 (2008).
12. Alam, P., Bousset, L., Melki, R. & Otzen, D. E. Alpha-synuclein oligomers and fibrils: a spectrum of species, a spectrum of toxicities. *J. Neurochem.* **150**, 522–534 (2019).
13. Marotta, N. P. & Lee, V. M. Modeling the cellular fate of alpha-synuclein aggregates: a pathway to pathology. *Curr. Opin. Neurobiol.* **72**, 171–177 (2022).
14. Volpicelli-Daley, L. & Brundin, P. Prion-like propagation of pathology in Parkinson disease. *Handb. Clin. Neurol.* **153**, 321–335 (2018).
15. Jan, A., Goncalves, N. P., Vaegter, C. B., Jensen, P. H. & Ferreira, N. The prion-like spreading of alpha-synuclein in Parkinson's disease: update on models and hypotheses. *Int. J. Mol. Sci.* **22** https://doi.org/10.3390/ijms22158338 (2021).
16. Polinski, N. K. A summary of phenotypes observed in the in vivo rodent alpha-synuclein preformed fibril model. *J. Parkinsons Dis.* **11**, 1555–1567 (2021).
17. Fares, M. B., Jagannath, S. & Lashuel, H. A. Reverse engineering Lewy bodies: how far have we come and how far can we go?. *Nat. Rev. Neurosci.* **22**, 111–131 (2021).
18. Henderson, M. X. et al. Spread of alpha-synuclein pathology through the brain connectome is modulated by selective vulnerability and predicted by network analysis. *Nat. Neurosci.* **22**, 1248–1257 (2019).
19. Yang, Y. et al. Cryo-EM structures of α-synuclein filaments from Parkinson's disease and dementia with Lewy bodies. *bioRxiv* https://doi.org/10.1101/2022.07.12.499706 (2022).
20. Watts, J. C. et al. Transmission of multiple system atrophy prions to transgenic mice. *Proc. Natl Acad. Sci. USA* **110**, 19555–19560 (2013).
21. Ayers, J. I. et al. Different alpha-synuclein prion strains cause dementia with Lewy bodies and multiple system atrophy. *Proc. Natl Acad. Sci. USA* **119** https://doi.org/10.1073/pnas.2113489119 (2022).
22. Holec, S. A. M., Liu, S. L. & Woerman, A. L. Consequences of variability in alpha-synuclein fibril structure on strain biology. *Acta Neuropathol.* **143**, 311–330 (2022).
23. Melki, R. Disease mechanisms of multiple system atrophy: what a parallel between the form of pasta and the alpha-synuclein assemblies involved in MSA and PD tells us. *Cerebellum* https://doi.org/10.1007/s12311-022-01417-0 (2022).
24. Volpicelli-Daley, L. A. et al. Exogenous alpha-synuclein fibrils induce Lewy body pathology leading to synaptic dysfunction and neuron death. *Neuron* **72**, 57–71 (2011).
25. Bousset, L. et al. Structural and functional characterization of two alpha-synuclein strains. *Nat. Commun.* **4**, 2575 (2013).

26. Makky, A., Bousset, L., Polesel-Maris, J. & Melki, R. Nanomechanical properties of distinct fibrillar polymorphs of the protein alpha-synuclein. *Sci. Rep.* **6**, 37970 (2016).
27. Peelaerts, W. et al. alpha-Synuclein strains cause distinct synucleinopathies after local and systemic administration. *Nature* **522**, 340–344 (2015).
28. Van der Perren, A. et al. The structural differences between patient-derived alpha-synuclein strains dictate characteristics of Parkinson's disease, multiple system atrophy and dementia with Lewy bodies. *Acta Neuropathol.* **139**, 977–1000 (2020).
29. Peelaerts, W. & Baekelandt, V. a-Synuclein strains and the variable pathologies of synucleinopathies. *J. Neurochem.* **139**, 256–274 (2016).
30. Manzanza, N. O., Sedlackova, L. & Kalaria, R. N. Alpha-synuclein post-translational modifications: implications for pathogenesis of Lewy body disorders. *Front. Aging Neurosci.* **13**, 690293 (2021).
31. Sonustun, B. et al. Pathological relevance of post-translationally modified alpha-synuclein (pSer87, pSer129, nTyr39) in idiopathic Parkinson's disease and multiple system atrophy. *Cells* **11** https://doi.org/10.3390/cells11050906 (2022).
32. Kellie, J. F. et al. Quantitative measurement of intact alpha-synuclein proteoforms from post-mortem control and Parkinson's disease brain tissue by intact protein mass spectrometry. *Sci. Rep.* **4**, 5797 (2014).
33. Li, W. et al. Aggregation promoting C-terminal truncation of alpha-synuclein is a normal cellular process and is enhanced by the familial Parkinson's disease-linked mutations. *Proc. Natl Acad. Sci. USA* **102**, 2162–2167 (2005).
34. Moors, T. E. et al. The subcellular arrangement of alpha-synuclein proteoforms in the Parkinson's disease brain as revealed by multicolor STED microscopy. *Acta Neuropathol.* **142**, 423–448 (2021).
35. Sorrentino, Z. A. et al. Physiological C-terminal truncation of alpha-synuclein potentiates the prion-like formation of pathological inclusions. *J. Biol. Chem.* **293**, 18914–18932 (2018).
36. Michell, A. W. et al. The effect of truncated human alpha-synuclein (1-120) on dopaminergic cells in a transgenic mouse model of Parkinson's disease. *Cell Transpl.* **16**, 461–474 (2007).
37. Masliah, E. et al. Passive immunization reduces behavioral and neuropathological deficits in an alpha-synuclein transgenic model of Lewy body disease. *PLoS ONE* **6**, e19338 (2011).
38. Bergstrom, A. L., Kallunki, P. & Fog, K. Development of passive immunotherapies for synucleinopathies. *Mov. Disord.* **31**, 203–213 (2016).
39. Schneeberger, A., Tierney, L. & Mandler, M. Active immunization therapies for Parkinson's disease and multiple system atrophy. *Mov. Disord.* **31**, 214–224 (2016).
40. Pagano, G. T. et al. A Phase II study to evaluate the safety and efficacy of prasinezumab in Early Parkinson's disease (PASADENA): rationale, design, and baseline data. *Front. Neurol.* **12**, 705407 (2021).
41. Pagano, G. et al. Trial of prasinezumab in early-stage Parkinson's disease. *N. Engl. J. Med.* **387**, 421–432 (2022).
42. Lang, A. E. et al. Trial of cinpanemab in early Parkinson's disease. *N. Engl. J. Med.* **387**, 408–420 (2022).
43. Nordstrom, E. et al. ABBV-0805, a novel antibody selective for soluble aggregated alpha-synuclein, prolongs lifespan and prevents buildup of alpha-synuclein pathology in mouse models of Parkinson's disease. *Neurobiol. Dis.* **161**, 105543 (2021).
44. Fjord-Larsen, L. et al. Nonclinical safety evaluation, pharmacokinetics, and target engagement of Lu AF82422, a monoclonal IgG1 antibody against alpha-synuclein in development for treatment of synucleinopathies. *MAbs* **13**, 1994690 (2021).
45. Poewe, W. et al. Safety and tolerability of active immunotherapy targeting alpha-synuclein with PD03A in patients with early Parkinson's disease: a randomized, placebo-controlled, phase 1 study. *J. Parkinsons Dis.* **11**, 1079–1089 (2021).
46. Levin, J. et al. Safety, tolerability and pharmacokinetics of the oligomer modulator anle138b with exposure levels sufficient for therapeutic efficacy in a murine Parkinson model: a randomised, double-blind, placebo-controlled phase 1a trial. *EBioMedicine* **80**, 104021 (2022).
47. Cole, T. A. et al. alpha-Synuclein antisense oligonucleotides as a disease-modifying therapy for Parkinson's disease. *JCI Insight* **6** https://doi.org/10.1172/jci.insight.135633 (2021).
48. Durocher, Y., Perret, S. & Kamen, A. High-level and high-throughput recombinant protein production by transient transfection of suspension-growing human 293-EBNA1 cells. *Nucleic Acids Res.* **30**, E9 (2002).
49. Vink, T., Oudshoorn-Dickmann, M., Roza, M., Reitsma, J. J. & de Jong, R. N. A simple, robust and highly efficient transient expression system for producing antibodies. *Methods* **65**, 5–10 (2014).
50. Acierno, J. P., Braden, B. C., Klinke, S., Goldbaum, F. A. & Cauerhff, A. Affinity maturation increases the stability and plasticity of the Fv domain of anti-protein antibodies. *J. Mol. Biol.* **374**, 130–146 (2007).
51. Burton, D. R. et al. Efficient neutralization of primary isolates of HIV-1 by a recombinant human monoclonal antibody. *Science* **266**, 1024–1027 (1994).
52. Tarutani, A., Arai, T., Murayama, S., Hisanaga, S. I. & Hasegawa, M. Potent prion-like behaviors of pathogenic alpha-synuclein and evaluation of inactivation methods. *Acta Neuropathol. Commun.* **6**, 29 (2018).
53. Battye, T. G., Kontogiannis, L., Johnson, O., Powell, H. R. & Leslie, A. G. iMOSFLM: a new graphical interface for diffraction-image processing with MOSFLM. *Acta Crystallogr. D. Biol. Crystallogr.* **67**, 271–281 (2011).
54. Evans, P. R. & Murshudov, G. N. How good are my data and what is the resolution?. *Acta Crystallogr. D. Biol. Crystallogr.* **69**, 1204–1214 (2013).
55. Emsley, P., Lohkamp, B., Scott, W. G. & Cowtan, K. Features and development of Coot. *Acta Crystallogr. D. Biol. Crystallogr.* **66**, 486–501 (2010).
56. McCoy, A. J. et al. Phaser crystallographic software. *J. Appl. Crystallogr.* **40**, 658–674 (2007).
57. Vagin, A. A. et al. REFMAC5 dictionary: organization of prior chemical knowledge and guidelines for its use. *Acta Crystallogr. D. Biol. Crystallogr.* **60**, 2184–2195 (2004).
58. Chen, W. et al. Accurate calculation of relative binding free energies between ligands with different net charges. *J. Chem. Theory Comput.* **14**, 6346–6358 (2018).
59. Clark, A. J. et al. Relative binding affinity prediction of charge-changing sequence mutations with FEP in protein-protein interfaces. *J. Mol. Biol.* **431**, 1481–1493 (2019).
60. Wang, L., Berne, B. J. & Friesner, R. A. On achieving high accuracy and reliability in the calculation of relative protein-ligand binding affinities. *Proc. Natl Acad. Sci. USA* **109**, 1937–1942 (2012).
61. Wang, L. et al. Accurate and reliable prediction of relative ligand binding potency in prospective drug discovery by way of a modern free-energy calculation protocol and force field. *J. Am. Chem. Soc.* **137**, 2695–2703 (2015).
62. Westerlund, M. et al. Lrrk2 and alpha-synuclein are co-regulated in rodent striatum. *Mol. Cell Neurosci.* **39**, 586–591 (2008).
63. Luk, K. C. et al. Pathological alpha-synuclein transmission initiates Parkinson-like neurodegeneration in nontransgenic mice. *Science* **338**, 949–953 (2012).
64. Schweighauser, M. et al. Structures of alpha-synuclein filaments from multiple system atrophy. *Nature* **585**, 464–469 (2020).
65. Yang, Y. et al. Structures of alpha-synuclein filaments from human brains with Lewy pathology. *Nature* **610**, 791–795 (2022).
66. Jankovic, J. et al. Safety and tolerability of multiple ascending doses of PRX002/RG7935, an anti-alpha-synuclein monoclonal antibody, in patients with Parkinson disease: a randomized clinical trial. *JAMA Neurol.* **75**, 1206–1214 (2018).

67. Weihofen, A. et al. Development of an aggregate-selective, human-derived alpha-synuclein antibody BIIB054 that ameliorates disease phenotypes in Parkinson's disease models. *Neurobiol. Dis.* **124**, 276–288 (2019).
68. Kumar, S. T. et al. Characterization and validation of 16 α-synuclein conformation-specific antibodies using well-characterized preparations of α-synuclein monomers, fibrils and oligomers with distinct structures and morphology: How specific are the conformation-specific α-synuclein antibodies? *bioRxiv* https://doi.org/10.1101/2020.06.15.151514 (2020).
69. Linse, S. et al. Kinetic fingerprints differentiate the mechanisms of action of anti-Abeta antibodies. *Nat. Struct. Mol. Biol.* **27**, 1125–1133 (2020).
70. Mahul-Mellier, A. L. et al. The process of Lewy body formation, rather than simply alpha-synuclein fibrillization, is one of the major drivers of neurodegeneration. *Proc. Natl Acad. Sci. USA* **117**, 4971–4982 (2020).
71. Parra-Rivas, L. A. et al. Serine-129 phosphorylation of alpha-synuclein is an activity-dependent trigger for physiologic protein-protein interactions and synaptic function. *Neuron* **111**, 4006–4023.e4010 (2023).
72. Wu, Q. et al. Neuronal activity modulates alpha-synuclein aggregation and spreading in organotypic brain slice cultures and in vivo. *Acta Neuropathol.* **140**, 831–849 (2020).
73. Ueda, J. et al. Perampanel inhibits alpha-synuclein transmission in Parkinson's disease models. *Mov. Disord.* **36**, 1554–1564 (2021).
74. Barth, M. et al. Microglial inclusions and neurofilament light chain release follow neuronal alpha-synuclein lesions in long-term brain slice cultures. *Mol. Neurodegener.* **16**, 54 (2021).
75. Okuda, S. et al. Rapid induction of dopaminergic neuron loss accompanied by Lewy body-like inclusions in A53T BAC-SNCA transgenic mice. *Neurotherapeutics* **19**, 289–304 (2022).
76. Sorrentino, Z. A. & Giasson, B. I. The emerging role of alpha-synuclein truncation in aggregation and disease. *J. Biol. Chem.* **295**, 10224–10244 (2020).
77. Hass, E. W. et al. Disease-, region- and cell type specific diversity of alpha-synuclein carboxy terminal truncations in synucleinopathies. *Acta Neuropathol. Commun.* **9**, 146 (2021).
78. Schofield, D. J. et al. Preclinical development of a high affinity alpha-synuclein antibody, MEDI1341, that can enter the brain, sequester extracellular alpha-synuclein and attenuate alpha-synuclein spreading in vivo. *Neurobiol. Dis.* **132**, 104582 (2019).
79. Buur, L. et al. Randomized phase I trial of the alpha-synuclein antibody Lu AF82422. *Mov. Disord.* https://doi.org/10.1002/mds.29784 (2024).
80. Kuchimanchi, M., Monine, M., Kandadi Muralidharan, K., Woodward, C. & Penner, N. Phase II dose selection for alpha synuclein-targeting antibody cinpanemab (BIIB054) based on target protein binding levels in the brain. *CPT Pharmacomet. Syst. Pharm.* **9**, 515–522 (2020).
81. Geerts, H., Bergeler, S., Walker, M., van der Graaf, P. H. & Courade, J. P. Analysis of clinical failure of anti-tau and anti-synuclein antibodies in neurodegeneration using a quantitative systems pharmacology model. *Sci. Rep.* **13**, 14342 (2023).
82. Rahayel, S. et al. Differentially targeted seeding reveals unique pathological alpha-synuclein propagation patterns. *Brain* **145**, 1743–1756 (2022).
83. Hansen, M. L. et al. Characterization of pSer129-alphaSyn pathology and neurofilament light-chain release across in vivo, ex vivo, and in vitro models of pre-formed-fibril-induced alphaSyn aggregation. *Cells* **13** https://doi.org/10.3390/cells13030253 (2024).
84. Knecht, L., Folke, J., Dodel, R., Ross, J. A. & Albus, A. Alpha-synuclein immunization strategies for synucleinopathies in clinical studies: a biological perspective. *Neurotherapeutics* https://doi.org/10.1007/s13311-022-01288-7 (2022).
85. Brys, M. et al. Randomized phase I clinical trial of anti-alpha-synuclein antibody BIIB054. *Mov. Disord.* **34**, 1154–1163 (2019).
86. Siderowf, A. et al. Assessment of heterogeneity among participants in the Parkinson's Progression Markers Initiative cohort using alpha-synuclein seed amplification: a cross-sectional study. *Lancet Neurol.* **22**, 407–417 (2023).
87. Shahnawaz, M. et al. Discriminating alpha-synuclein strains in Parkinson's disease and multiple system atrophy. *Nature* **578**, 273–277 (2020).
88. Singer, W. et al. Alpha-synuclein oligomers and neurofilament light chain predict phenoconversion of pure autonomic failure. *Ann. Neurol.* **89**, 1212–1220 (2021).
89. Majbour, N. et al. Disease-associated alpha-synuclein aggregates as biomarkers of Parkinson disease clinical stage. *Neurology* **99**, e2417–e2427 (2022).
90. Desai, A. A. et al. Flow cytometric isolation of drug-like conformational antibodies specific for amyloid fibrils. *bioRxiv* https://doi.org/10.1101/2023.07.04.547698 (2023).
91. Moors, T. E. et al. Multi-platform quantitation of alpha-synuclein human brain proteoforms suggests disease-specific biochemical profiles of synucleinopathies. *Acta Neuropathol. Commun.* **10**, 82 (2022).

Acknowledgements

Rikke Madsen, Nikki Jane Damsgaard, Nancy Mutsaers, Anja Lau Schiöpffe, Nils Sørensen, Bo Albrechtslund, Rie Christensen, Camilla Thormod Hjort, Evin Turan, Karina Lynge Laursen, Susanne Kristine Lüder, Lene Skrubbeltrang.

Author contributions

Pekka Kallunki: project administration, experimental designs, in vitro histology, protein binding using MDS, analysis of histology data from human brain sections, and writing of original draft. Florence Sotty: experimental design of in vivo experiments, in vivo histology data analysis and statistical analysis. Katarina Willén, Ann-Louise Bergström, Malene Ambjørn, Thomas Thiilmark Eriksen and Ibrahim Malik: investigation using in vitro cellular models, antibody screening, data analysis. Michal Lubas and Louise Buur: characterization of antibody binding to brain extracts by immunoprecipitation. Laurent David and Kaare Bjerregaard-Andersen: generation and analysis of crystal structure data. Steffen Nyegaard, Kaare Bjerregaard-Andersen, and Ersoy Cholak: α-syn assembly generation and qualification, α-syn aggregate purification from human brains. Berit O. Krogh: antibody generation and affinity analysis on monomer α-syn. Lars Ø. Pedersen: characterization of antibody binding to brain extracts by quantitative ELISA. Pernille Gry Wulff-Larsen, Sandra Vergo, Josefine N. Søderberg, Mikkel N. Harndahl and Dina S. M. Damlund: analysis of antibody affinity and avidity on α-syn monomers and fibrillar assemblies and aggregates. Kathrine J. Andersen: analysis of antibody data from in vivo models, PK analysis. Line R. Olsen: PK measurement and data analysis. Søren Christensen and Mikkel N. Harndahl: antibody generation. Edward N. van den Brink, Rik Rademaker, David Satijn, Paul W.H.I. Parren, Jeffrey B. Stavenhagen and Jan Egebjerg: led antibody campaign at Lundbeck and Genmab. Allan Jensen: led antibody generation and analysis at Lundbeck. Kaare Bjerregaard-Andersen: protein and antibody generation, data analysis and writing of original draft. Karina Fog: conceptualization, experimental designs, data analysis and writing of original draft.

Competing interests

P.K., F.S., K.W., M.L., L.D., M.A., L.B., B.O.K., L.R.O., S.V., A.J., M.N.H., D.S.M.D., K.B.-A., K.F. are full-time employees of H. Lundbeck A/S. A.-L.B., I.M., S.N., T.T.E., J.B.S., K.J.A., L.Ø.P., S.C., J.E., J.N.S., P.G.W.-L. were full-time employees of H. Lundbeck A/S at the time of this work. E.N.V.D.B., R.R., D.S., P.P. were full-time employees of Genmab BV at the time of this work. The research was funded by H. Lundbeck A/S, Copenhagen, Denmark.

Additional information

Supplementary information The online version contains supplementary material available at https://doi.org/10.1038/s41531-024-00849-1.

Correspondence and requests for materials should be addressed to Pekka Kallunki.